Rational Design and Assembly of $M_2M'_3L_6$ Supramolecular Clusters with C_{3h} Symmetry by Exploiting Incommensurate Symmetry Numbers§

Xiankai Sun,† Darren W. Johnson,‡ Dana L. Caulder,‡ Kenneth N. Raymond,*,‡ and Edward H. Wong*,†

Contribution from the Departments of Chemistry, University of New Hampshire, Durham, New Hampshire 03824, and University of California, Berkeley, California 94720-1460

Received August 7, 2000

Abstract: A rational approach to heterometallic cluster formation is described that uses incommensurate symmetry requirements at two different metals to control the stoichiometry of the assembly. Critical to this strategy is the proper design and synthesis of hybrid ligands with coordination sites selective toward each metal. The phosphino-catechol ligand 4-(diphenylphosphino)benzene-1,2-diol (H_2**L**) possesses both hard catecholate and soft phosphine donor sites and serves such a role, using soft (C_2-symmetric) and hard (C_3-symmetric) metal centers. The ML_3 catecholate complexes (M = Fe^{III}, Ga^{III}, Ti^{IV}, Sn^{IV}) have been prepared and characterized as C_3-symmetry precursors for the stepwise assembly (*aufbau)* of heterometallic clusters. While the single-crystal X-ray structure of the Cs_2[Ti**L**$_3$] salt shows a C_1 *mer*-configuration in the solid -state, room-temperature solution NMR data of this and related complexes are consistent with either exclusive formation of the C_3-*fac*-isomer with all PPh_2 donor sites *syn* to each other or facile *fac/mer* isomerization. Coordination of these $[M\mathbf{L}_3]^{2-}$ (M = Ti^{IV}, Sn^{IV}) metallaligands via their soft P donor sites to C_2-symmetric $PdBr_2$ units gives exclusively pentametallic $[M_2Pd_3Br_6\mathbf{L}_6]^{4-}$ (M = Ti, Sn) clusters. These clusters have been fully characterized by spectral and X-ray structural data as C_{3h} mesocates with Cs^+ or protonated 1,4-diazabicyclo-[2.2.2]octane (DABCO·H^+) cations incorporated into deep molecular clefts. Exclusive formation of this type of supramolecular species is sensitive to the nature of the counterions. Alkali cations such as K^+, Rb^+, and Cs^+ give high-yield formation of the respective clusters while NEt_3H^+ and NMe_4^+ yield none of the desired products. Extension of the *aufbau* assembly to produce related $[M_2Pd_3Cl_6\mathbf{L}_6]^{4-}$, $[M_2Pd_3I_6\mathbf{L}_6]^{4-}$, and $[M_2Cr_3(CO)_{12}\mathbf{L}_6]^{4-}$ (M = Ti, Sn) clusters has also been realized. In addition to this *aufbau* approach, self-assembly of several of these $[M_2Pd_3Br_6\mathbf{L}_6]^{4-}$ clusters from all *eleven* components (two M^{IV}, three $PdBr_2$, six H_2**L**) was also accomplished under appropriate reaction conditions.

Introduction

The synthesis of high-symmetry metal−ligand clusters is an effective way to build large molecular constructs from small subunits. These clusters form spontaneously via self-assembly reactions from a mixture of labile components to yield the most thermodynamically stable product. Among a wide array of multinuclear supramolecular clusters, helicates and their *meso* counterparts (mesocates), rings, catenanes,[1,2] tetrahedra,[3] cylinders, cages,[4] octahedra, cubes, and icosahedra,[5] have been generated in this manner.[6−10] Much of this attention results from the intrinsic beauty of these clusters and the challenges in ligand design and cluster synthesis. However, many of these clusters exhibit fascinating properties as well, such as guest binding,[11−16]

* Authors to whom correspondence should be addressed. E-mail: ehw@christa.unh.edu, raymond@socrates.berkeley.edu.

§ Paper No. 19 in the series Coordination Number Incommensurate Cluster Formation. For the previous paper see: Terpin, A. J.; Ziegler, M.; Johnson, D. W.; Raymond, K. N. *Angew. Chem. Int. Ed.* **2000**, *39*, 157−160.

† University of New Hampshire, Durham.

‡ University of California, Berkeley.

(1) Sauvage, J. P. *Acc. Chem. Res.* **1998**, *31*, 611 and references therein.

(2) Fujita, M. *Acc. Chem. Res.* **1999**, *32*, 53 and references therein.

(3) Fox, O. D.; Drew, M. G. B.; Beer, P. D. *Angew. Chem., Int. Ed.* **2000**, *39*, 136.

(4) Takeda, N.; Umemoto, K.; Yamaguchi, K.; Fujita, M. *Nature* **1999**, *398*, 794.

(5) Olenyuk, B.; Whiteford, J. A.; Fechtenkotter, A.; Stang, P. J. *Nature* **1999**, *398*, 796.

(6) For all but the most recent papers on these molecules see the most thorough review in this field: Leininger, S.; Olenyuk, B.; Stang, P. J. *Chem. Rev.* **2000**, *100*, 853. For applications see pp 902−903.

(7) Piguet, C.; Bernardinelli, G.; Hopfgartner, G. *Chem. Rev.* **1997**, *97*, 2005 and references therein.

(8) Lehn, J.-M. *Supramolecular Chemistry: Concepts and Perspectives*; VCH: Weinheim, 1995, and references therein.

(9) Raymond, K. N.; Caulder, D. L.; Powers, R. E.; Beissel, T.; Meyer, M.; Kersting, B. *Proc. 40th Robert A. Welch Found. Chem. Res.* **1996**, *40*, 115 and references therein.

(10) (a) Caulder, D. L.; Raymond, K. N. *J. Chem. Soc., Dalton Trans.* **1998**, 1185 and references therein. (b) Saalfrank, R. W.; Demleitner, B. In *Transition Metals in Supramolecular Chemistry*; Sauvage, J.-P., Ed.; John Wiley & Sons Ltd.: Chichester, England, 1999; Perspectives in Supramolecular Chemistry, Vol. 5, pp 1−51 and references therein.

(11) Fleming, J. S.; Mann, K. L. V.; Carraz, C.-A.; Psillakis, E.; Jeffery, J. C.; McCleverty, J. A.; Ward, M. D. *Angew. Chem., Int. Ed.* **1998**, *37*, 1279.

(12) Gokel, G. W. *Molecular Recognition: Receptors for Cationic Guests*; Pergamon: New York, 1996; Vol. 1 and references therein.

(13) Aoyagi, M.; Biradha, K.; Fujita, M. *J. Am. Chem. Soc.* **1999**, *121*, 7457.

(14) Kusukawa, T.; Fujita, M. *J. Am. Chem. Soc.* **1999**, *121*, 1397.

(15) Parac, T.; Caulder, D. L.; Raymond, K. N. *J. Am. Chem. Soc.* **1998**, *120*, 8003.

10.1021/ja0029376 CCC: $20.00
Published on Web 02/22/2001

chiral resolution,[17−21] dynamic interconversion of assemblies,[22−25] mechanical coupling between metal centers,[26−28] catalysis,[29] and magnetism,[30−33] inter alia.[6]

We have developed a predictive design strategy[10] resulting in the synthesis of various high-symmetry coordination clusters including M_2L_3 helicates[26,34,35] and mesocates,[22,36] M_4L_6[25,28,37,38] and M_4L_4 tetrahedra,[39] M_6L_6[40] and M_8L_8 cylinders, and M_8L_6 octahedra.[41] These examples all focus on the coordination of three bidentate chelators to a tri- or tetravalent metal ion in a pseudooctahedral fashion at the apexes of the clusters. This coordination generates local 3-fold symmetry at these metal centers. These chelators are contained in a rigid, symmetric multi(bidentate)-ligand, which supplies the other symmetry elements of the cluster (2-fold, 3-fold, or mirror plane). By simultaneously fulfilling the symmetry requirements of both the ligand and metal centers, discrete high-symmetry clusters are generated under thermodynamic control.

Recently, we communicated the stepwise assembly of two $M_2M'_3L_6$ mesocates in which a second type of metal ion, rather than a symmetric ligand, supplies the mirror plane symmetry in the cluster.[36] In principle, the ligand forms part of an asymmetric unit of the cluster and must have two different interaction sites (e.g., one hard and one soft donor) that can each preferentially interact with one of the metal ions over the other. Here we present details of both this stepwise assembly as well as the *spontaneous self-assembly* from all 11 components of a series of mesocates from such an asymmetric "hybrid", wherein two *different metals* are used to generate the two incommensurate symmetry elements of the clusters (Figure 1). This use of incommensurate metal−ligand interactions forms the basis for our design strategy. Full synthetic details and discussions on several single-crystal X-ray structures are also presented.

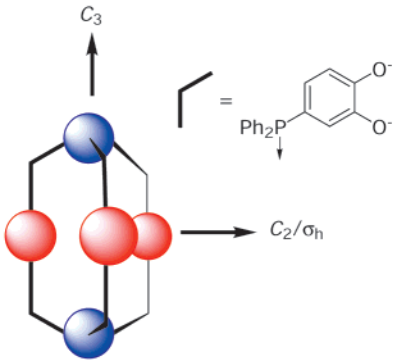

Figure 1. Cartoon showing the 90° offset, incommensurate interaction of a 3-fold symmetry element (blue spheres), and a C_2 axis/mirror plane (red spheres) linked by a hybrid ligand **L** (black) to generate a $M_2M'_3L_6$ cluster.

Results and Discussion

Ligand Design. The assembly of a mixed-metal helicate of the type $Ru_2Cu_3L_6$ was recently reported where a substitution-inert Ru^{II}[3-(pyridin-2-yl)pyrazole]$_3$ complex was used as the 3-fold interaction site.[42] The uncoordinated nitrogen atom of the pyrazole ring remains free to coordinate labile Cu^{I} to generate a 2-fold axis and thus assemble a triple helicate. We chose to explore the use of a hybrid ligand with more distinguishing coordination sites, namely catechol and phosphine. Catechol is a hard chelating ligand that generates a C_3 axis when coordinated to hard, tri- or tetravalent metals with preferred octahedral coordination (e.g., Al^{III}, Ga^{III}, Fe^{III}, Sn^{IV}, Ti^{IV}).[43,44] Phosphine ligands, on the other hand, are soft donors which can coordinate to square-planar metals (e.g., Pd^{II} or Pt^{II}) in a *trans* fashion to generate a 2-fold axis or mirror plane.[45,46] A properly designed hybrid ligand containing both these donors could assemble an $M_2M'_3L_6$ cluster, the smallest discrete species that would simultaneously fulfill the two orthogonal symmetry requirements. Molecular models (CAChe[47]) suggested a 4-phosphinocatechol ligand (Figure 2) would have the ideal geometry for isolating the two types of coordination sites and to permit cluster assembly.

Synthesis and Characterization of the Hybrid Ligand H_2L. The hybrid ligand H_2**L** can be readily prepared in two steps from 4-dichlorophosphino-veratrole (Scheme 1). The latter was obtained from veratrole under Friedel−Crafts conditions by using a literature synthesis.[48] Grignard reaction of 4-dichlorophosphino-veratrole with phenylmagnesium bromide afforded

(16) Saalfrank, R. W.; Burak, R.; Breit, A.; Stalke, D.; Herbst-Irmer, R.; Daub, J.; Porsch, M.; Bill, E.; Müther, M.; Trautwein, A. X. *Angew. Chem., Int. Ed.* **1994**, *33*, 1621.
(17) Knof, U.; von Zelewsky, A. *Angew. Chem., Int. Ed.* **1999**, *38*, 303.
(18) Krämer, R.; Lehn, J.-M.; DeCian, A.; Fischer, J. *Angew. Chem., Int. Ed.* **1993**, *32*, 703.
(19) Enemark, E. J.; Stack, T. D. P. *Angew. Chem., Int. Ed.* **1998**, *37*, 932.
(20) Stang, P. J.; Olenyuk, B.; Muddiman, D. C.; Smith, R. D. *Organomet.* **1997**, *16*, 3094.
(21) Masood, M. A.; Enemark, E. J.; Stack, T. D. P. *Angew. Chem., Int. Ed.* **1998**, *37*, 928.
(22) Xu, J.; Parac, T.; Raymond, K. N. *Angew. Chem., Int. Ed.* **1999**, *19*, 2878.
(23) Lee, S. B.; Hwang, S.; Chung, D. S.; Yun, H.; Hong, J.-I. *Tetrahedron Lett.* **1998**, *39*, 873.
(24) Hasenknopf, B.; Lehn, J.-M.; Kneisel, B. O.; Baum, G.; Fenske, D. *Angew. Chem., Int. Ed.* **1996**, *35*, 1838.
(25) Scherer, M.; Caulder, D. L.; Johnson, D. W.; Raymond, K. N. *Angew. Chem., Int. Ed.* **1999**, *38*, 1588.
(26) Kersting, B.; M. Meyer; Powers, R. E.; Raymond, K. N. *J. Am. Chem. Soc.* **1996**, *118*, 7221.
(27) Pfeil, A.; Lehn, J.-M. *Chem. Commun.* **1992**, 838.
(28) Beissel, T.; Powers, R. E.; Parac, T. N.; Raymond, K. N. *J. Am. Chem. Soc.* **1999**, *121*, 4200.
(29) Sanders, J. K. M. *Chem. Eur. J.* **1998**, *4*, 1378.
(30) Waldmann, O.; Schulein, J.; Koch, A.; Muller, P.; Bernt, I.; Saalfrank, R. W.; Andres, H. P.; Gudel, H. U.; Allenspach, P. *Inorg. Chem.* **1999**, *38*, 5879.
(31) Gatteschi, D.; Caneschi, A.; Pardi, L.; Sessoli, R. *Science* **1994**, *265*, 1054.
(32) Amoroso, A. J.; Jeffery, J. C.; Jones, P. L.; McCleverty, J. A.; Thornton, P.; Ward, M. D. *Angew. Chem., Int. Ed.* **1995**, *34*, 1443.
(33) Taft, K. L.; Delfs, C. D.; Papaefthymiou, G. C.; Foner, S.; Gatteschi, D.; Lippard, S. J. *J. Am. Chem. Soc.* **1994**, *116*, 823.
(34) Kersting, B.; Telford, J. R.; Meyer, M.; Raymond, K. N. *J. Am. Chem. Soc.* **1996**, *118*, 5712.
(35) Caulder, D. L.; Raymond, K. N. *Angew. Chem., Int. Ed.* **1997**, *36*, 1439.
(36) Sun, X.; Johnson, D. W.; Caulder, D. L.; Powers, R. E.; Raymond, K. N.; Wong, E. H. *Angew. Chem.* **1999**, *38*, 1303.
(37) Caulder, D. L.; Powers, R. E.; Parac, T.; Raymond, K. N. *Angew. Chem., Int. Ed.* **1998**, *37*, 1840.
(38) Beissel, T.; Powers, R. E.; Raymond, K. N. *Angew. Chem., Int. Ed.* **1996**, *35*, 1084.
(39) Brückner, C.; Powers, R. E.; Raymond, K. N. *Angew. Chem., Int. Ed.* **1998**, *37*, 1837.
(40) Johnson, D. W.; Xu, J.; Saalfrank, R. W.; Raymond, K. N. *Angew. Chem., Int. Ed.* **1999**, *38*, 2882.
(41) Xu, J.; Raymond, K. N. **2000**, manuscript in preparation.
(42) Lam, M. H. W.; Cheung, S. T. C.; Fung, K.-M.; Wong, W.-T. *Inorg. Chem.* **1997**, *36*, 4618.
(43) Pierpoint, C. G.; Buchanan, R. M. *Coord. Chem. Rev.* **1981**, *38*, 45.
(44) Pierpoint, C. G.; Lange, C. W. *Inorg. Chem.* **1994**, *33*, 331.
(45) McAuliffe, C. A.; Wilkinson, G.; Stone, F. G. A.; Abel, F. W., Eds.; Pergamon: Oxford, 1987; Vol. 2, Chapter 14.
(46) Levason, W.; Hartley, F. R., Ed.; Wiley: New York, 1990; Vol. 1, pp Chapter 16.
(47) *CAChe*, Version 4.0; Oxford Molecular Group, Inc., U.S.A., 1997.
(48) Miles, J. A.; Beeny, M. T.; Ratts, K. W. *J. Org. Chem.* **1975**, *40*, 343.

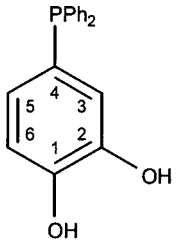

H_2**L**

Figure 2. The 4-phosphino-catechol hybrid ligand.

Scheme 1

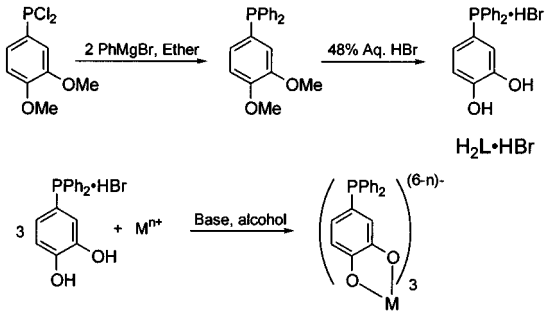

4-diphenylphosphino-veratrole in 70−80% yield as a white solid. Demethylation with 48% aqueous HBr yielded a white precipitate of H_2**L**·HBr. This was recrystallized from ethanol with 48% aqueous HBr to give analytically pure H_2**L**·HBr in 70% yield. The proton NMR spectrum of this ligand in d_7-DMF revealed three well-resolved multiplets for the catechol protons: two doublet of doublets and a higher field triplet of doublets. Assignment of these as H(6), H(3), and H(5) respectively was made based on spectral simulation and selective irradiation experiments (Figure 2). The catechol resonances in the $^{13}C\{^1H\}$ NMR spectrum were also well-resolved with the six unique ring carbons ranging from δ 147.7 to 116.6 (see Experimental Section). $^{31}P-^{13}C$ couplings were observable for all resonances except that of C(1) which is *para* to the PPh_2 substituent.

Syntheses and Characterization of $[ML_3]^{n-}$ Complexes. The isolation of the soft phosphine donor site from the hard dianionic catecholate chelate, crucial to our ligand design, ensures that the ligand will bridge two metal centers when fully coordinated, rather than forming a single metal complex using both donor sets. While hard metal cations can exclusively bind at the catecholate site, softer metal centers may not discriminate sufficiently between phosphine and catecholate coordination modes. Thus Pd^{II}, for example, reacted with H_2**L** to give an insoluble and intractable brown solid. This is presumably an oligomeric or polymeric product containing indiscriminate P and catecholate coordination to each Pd^{II} center. Exclusive bonding of soft metals to the P site may eventually be realized indirectly by first forming the 4-PPh_2-veratrole complex with subsequent deprotection of the methoxy groups under mild conditions.[49−51] Thus we opted to form the catecholate complex first. Harder tri- and tetravalent metals such as Al^{III}, Ga^{III}, Fe^{III}, Ti^{IV}, and Sn^{IV} reacted smoothly under basic conditions with H_2**L**·HBr to give tris-catecholate complexes without interference from the P-donor groups. Thus $[ML_3]^{3-}$ (M = Fe, Ga) and $[ML_3]^{2-}$ (M = Ti, Sn) were synthesized in good yields according to Scheme 1. These products were characterized by elemental and spectral analyses. Their IR spectra all show a common strong catecholate C−O band at ca. 1260 cm^{-1}, diagnostic of the coordinated catecholate groups.[52,53] While the Fe^{III} complex is dark red in color, the Ti^{IV} complex is red-orange, and the Ga^{III} and Sn^{IV} complexes are both white solids. The electronic spectrum of the Cs_3Fe**L**$_3$ complex in methanol solution exhibited a LMCT λ_{max} at 490 nm (ϵ = 6050 L cm^{-1} mol^{-1}).[54,55] EPR spectra of the Cs_3Fe**L**$_2$ complex in the solid state or in methanol solution at room temperature both exhibited a major g = 4.25 signal typical of high-spin ferric catecholate complexes.[55] The trianionic complexes were considerably more air-sensitive than the dianionic complexes, with partial air oxidation of the PPh_2 groups evident after overnight exposure.

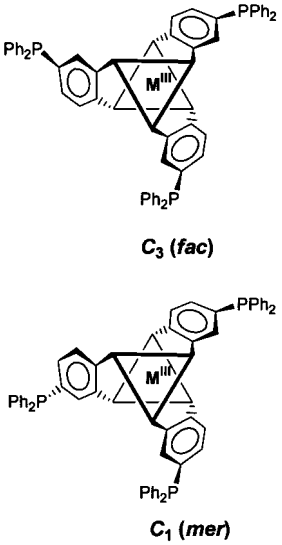

Figure 3. Depiction of the *fac*- and *mer*-isomers of Λ-$[ML_3]^{n-}$.

As anticipated, the PPh_2 groups were found to remain uncoordinated in accord with the observed $^{31}P\{^1H\}$ singlet chemical shifts (δ −2.0 to −6.0) in the three diamagnetic Ga^{III}, Ti^{IV}, and Sn^{IV} $[ML_3]^{n-}$ complexes.[56,57] Further, room temperature solution ^1H and $^{13}C\{^1H\}$ NMR data of these products all exhibited a single set of ligand catecholate and phenyl resonances indicative of C_3 symmetry. This is consistent with either exclusive formation of the *fac*-isomer or rapid isomerization involving the *mer*-isomer of C_1 symmetry (Figure 3). All three catecholate proton resonances shifted upfield upon metal complexation by 0.26 ppm up to 0.73 ppm, as previously observed for Ga^{III} and Rh^{III} tris-catecholate complexes.[58,59] Significant ^{13}C coordination shifts were found for the catechol

(49) Sembering, S. B.; Colbran, S. B.; Craig, D. C. *Inorg. Chem.* **1995**, *34*, 761.
(50) Sembering, S. B.; Colbran, S. B.; Craig, D. C.; Scudder, M. L. *J. Chem. Soc., Dalton Trans.* **1995**, 3731.
(51) Sembiring, S. B.; Colbran, S. B.; Craig, D. C. *J. Chem. Soc., Dalton Trans.* **1999**, 1543.
(52) Sofen, S. R.; Abu-Dari, K.; Freyberg, D. P.; Raymond, K. N. *J. Am. Chem. Soc.* **1978**, *100*, 7882.
(53) Griffith, W. P.; Pumphrey, C. A.; Rainey, T.-A. **1986**, 1125.
(54) Karpishin, T. B.; Gebhard, M. S.; Solomon, E. I.; Raymond, K. N. *J. Am. Chem. Soc.* **1991**, *113*, 2977.
(55) Avdeef, A.; Sofen, S. R.; Bregante, T. L.; Raymond, K. N. *J. Am. Chem. Soc.* **1978**, *100*, 5362.
(56) Gorenstein, D. G. *Prog. NMR Spectrosc.* **1983**, *16*, 1.
(57) Quin, L. D.; Verkade, J. G. *Phosphorus-31 NMR Spectral Properties in Compound Characterization and Structural Analysis*; VCH: New York, 1994.
(58) McArdle, J. V.; Sofen, S. R.; Cooper, S. R.; Raymond, K. N. *Inorg. Chem.* **1978**, *17*, 3075.
(59) Linas, M.; Wilson, D. M.; Neilands, J. B. *Biochemistry* **1973**, *12*, 3835.

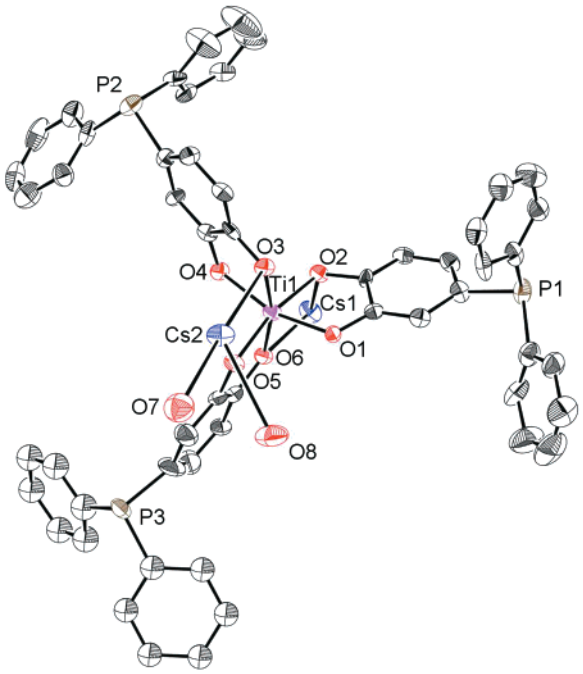

Figure 4. ORTEP of the solid-state structure of the $Cs_2[TiL_3]$ complex. For clarity only one of the two disordered PPh_2 groups (P(3)) is shown and only the oxygen atoms of coordinating solvents are shown (O(7) and O(8)). Thermal ellipsoids are at 50% probability.

Table 1. Selected Bond Distances (Å) and Bond Angles (deg) for $Cs_2[Ti(L)_3]$[a]

Cs(1)−O(2)	3.097(8)	O(1)−C(1)	1.35(2)
Cs(1)−O(2′)	3.305(7)	O(2)−C(2)	1.34(1)
Cs(1)−O(6)	3.051(8)	O(3)−C(19)	1.36(1)
Cs(1)−O(7)	3.21(1)	O(4)−C(20)	1.35(2)
Cs(1)−O(8)	3.11(1)	O(5)−C(37)	1.34(2)
Cs(2)−O(3)	3.164(8)	O(6)−C(38)	1.37(2)
Cs(2)−O(3′)	3.272(9)	O(7)−C(66)	1.26(2)
Cs(2)−O(5)	3.034(9)	O(8)−C(69)	1.10(4)
Cs(2)−O(7)	3.30(1)	P(1)−C(5)	1.83(1)
Cs(2)−O(8)	3.089(9)	P(1)−C(7)	1.84(1)
Ti(1)−O(1)	1.936(7)	P(1)−C(13)	1.87(1)
Ti(1)−O(2)	1.996(9)	P(2)−C(22)	1.81(1)
Ti(1)−O(3)	1.963(9)	P(2)−C(25)	1.82(1)
Ti(1)−O(4)	1.964(7)	P(2)−C(31)	1.82(1)
Ti(1)−O(5)	1.957(9)	P(3)−C(41)	1.84(2)
Ti(1)−O(6)	1.962(9)	P(3)−C(43)	1.86(2)
P(3)−C(61)	1.87(2)	P(4)−C(40)	1.92(3)
P(4)−C(49)	1.90(2)	P(4)−C(55)	1.92(3)
O(1)−Ti(1)−O(2)	79.8(3)	O(1)−Ti(1)−O(3)	88.5(3)
O(1)−Ti(1)−O(4)	162.8(4)	O(1)−Ti(1)−O(5)	92.8(3)
O(1)−Ti(1)−O(6)	103.1(3)	O(2)−Ti(1)−O(3)	98.6(4)
O(2)−Ti(1)−O(4)	89.3(3)	O(2)−Ti(1)−O(5)	166.8(3)
O(2)−Ti(1)−O(6)	90.0(4)	O(3)−Ti(1)−O(4)	80.0(3)
O(3)−Ti(1)−O(5)	92.0(4)	O(3)−Ti(1)−O(6)	166.7(4)
O(4)−Ti(1)−O(5)	100.2(3)	O(4)−Ti(1)−O(6)	90.1(3)
O(5)−Ti(1)−O(6)	81.1(4)		

[a] Primes represent symmetry equivalent atoms generated by the crystallographic inversion center.

ring carbons only. Both C(1) and C(2) were shifted sizably downfield by about 15 ppm upon metal coordination. Upfield shifts of over 5 ppm were observed for C(3), C(4), and C(6). Of the phenyl carbons, only the *ipso*-C shifted slightly, downfield by 1.8 ppm, again confirming the uncoordinated status of the PPh_2 moiety.

X-ray Structure of the $Cs_2[TiL_3]$ Complex. A single-crystal X-ray structural study of $Cs_2[TiL_3]\cdot 2DMF\cdot 0.5H_2O$ revealed a *mer* configuration in the solid state (Figure 4).[60] While P(1) and P(2) are in an *anti* configuration, the third phosphorus is disordered equally over two sites, giving a *mer* arrangement at either site.

The complex crystallizes as a racemic mixture of Δ and Λ configurations at the Ti centers. The average twist angle around Ti is 42.3°, indicative of an intermediate octahedral/trigonal prismatic coordination geometry. The six Ti−O bond lengths average to 1.96 Å with only Ti−O(1) and Ti−O(2) significantly different from the mean at 1.936(7) and 1.996(9) Å, respectively. Of the six catecholate oxygens only O(1) is not coordinated to a Cs cation, which may account for its short bond length to Ti. No clear trend in the existence of any *trans* influence on Ti−O or C−O bond lengths can be seen for the phenolic oxygens *meta* to or *trans* to the PPh_2 group. This is known to be a moderately electron-withdrawing substituent.[61,62] Similarly, no meaningful differences in the catcholate C−O distances, which average to 1.35 Å, were found.

The two cesium counterions are coordinated by catecholato oxygens as well as by dimethylformamide (DMF) solvent molecules. Each cation is coordinated by two catecholato oxygens and a third catecholato oxygen from an adjacent complex. In addition, Cs(2) is coordinated by one DMF and one disordered DMF or water solvent molecule, O(8) and O(7), respectively. On the other hand, Cs(1) is coordinated by such a solvent molecule from an adjacent complex. The Cs−O bond distances range from 3.034(9) Å for Cs(2)−O(5) to 3.305(7) Å for Cs(1)−O(2′). The intracomplex Cs···Cs separation is 5.176(2) Å. The surprisingly low coordination numbers of these cations are a direct result of the proximity of the phenyl substituents on the appended PPh_2 groups. In fact, each Cs cation is shielded from further solvation by a phenyl ring only 3.7 Å away. Other relevant bond distances and angles are listed in Table 1.

Configuration of the $[ML_3]^{2-}$ Complexes. In the absence of steric, electronic, ion-pairing, or solvation effects, the C_1 *mer* isomers of $[ML_3]^{2-}$ (M = Ti, Sn) and $[ML_3]^{3-}$ (M = Fe, Al, Ga) are statistically favored over the C_3 *fac* isomers by a 3:1 ratio. Of these, only the *fac* configuration has all three phosphino-donor groups disposed *syn* to each other, which is essential for successful formation of any endohedral metal cluster (Figure 3). While room temperature solution NMR data are fully consistent with either exclusive presence of this high-symmetry species in all cases or extremely facile *fac/mer* equilibration, the X-ray structure of $Cs_2[TiL_3]$ discussed above revealed a *mer* configuration in the solid state. We examined and discarded the possibility that the *fac* isomer is favored in solution due to steric, electronic, ion-pairing, and/or solvation factors.[63]

The alternative explanation for the observed high solution symmetry of ML_3^{2-} must be facile solution *fac/mer* isomerization processes that resulted in averaged spectra of C_3 symmetry. Extensive variable-temperature ^1H and $^{31}P\{^1H\}$ studies of TiL_3^{2-} and similar studies of SnL_3^{2-}, including ^{119}Sn NMR spectroscopy in a variety of solvents, failed to yield any unequivocal evidence for the slowing down of any *fac/mer* exchange. Literature data on fluxional behavior for Ti^{IV} and Sn^{IV} complexes with six-oxygen donors are relatively sparse.

(60) $Cs_2[TiL_3]\cdot 2DMF\cdot 0.5H_2O$: fragment of a red/yellow block, crystal size 0.30 × 0.07 × 0.07 mm^3, FW = 1345.73, T = −115 °C, triclinic space group, $P\bar{1}$, a = 11.4876(2) Å, b = 16.6820(3) Å, c = 16.7549(4) Å, α = 96.759(1)°, β = 99.298(1)°, γ = 98.647(1)°, V = 3099.3(1) $Å^3$, Z = 2, R = 0.064, Rw = 0.083, GOF = 2.13.

(61) van Doorn, J. *Phosphorus Sulfur* **1991**, *62*, 155.

(62) Louattani, E.; Lledos, A.; Suades, J.; Alvarez-Larena, A.; Piniella, J. F. *Organometallics* **1995**, *14*, 1053.

Fay and Lindmark[64,65] reported that both Ti^{IV} tris(β-diketonate) and bis(β-diketonate)$(OR)_2$ complexes of unsymmetrical ligands are fluxional down to −100 °C in methylene chloride solution. A recent review on Sn^{IV} bidentate oxygen donor chelates actually stated that tris(catecholate) Sn^{IV} complexes of unsymmetrically substituted catechols (e.g. 4-cyano, 4-methyl, 4-nitro, 4-chloro, etc.) exist as *fac/mer* mixtures in solution according to ^1H and ^{119}Sn NMR data.[66,67] This claim, however, appears to be unfounded.[68] Instead, only a single set of resonances was obtained in all the cases studied. The implication is that the dynamic behavior of Ti^{IV} and Sn^{IV} complexes with six oxygen donors may indeed be quite fast on the NMR time scale even at low temperatures. Possible acceleration of such dynamic processes by the presence of trace amounts of protons in our complexes can be ruled out since addition of *Proton Sponge* had no effect on the resulting spectra.

For our purposes, the successful synthesis of the desired C_{3h} pentametallic clusters mandates that the *fac* isomer *must* be accessible in solution whether due to its exclusive formation or through a facile *fac/mer* exchange.

Assembly of the $Cs_4[M_2Pd_3Br_6L_6]$ (M = Ti, Sn) Clusters. The $[ML_3]^{2-}$ complexes have three divergent diphenylphosphino groups that can coordinate to three separate metal centers (M′). If these metal centers are C_2 symmetric, supramolecular clusters of the type $M_2M'_3L_6$ (Figure 1) can be assembled. As monitored by $^{31}P\{^1H\}$ NMR spectroscopy, titration of 3 equiv of a DMF solution of $PdBr_2 \cdot 2PhCN$ into 2 equiv of $Cs_2[TiL_3]$ in DMF led to the exclusive formation of a single red product. No exchange between this complex with excess free ligand was observed on the NMR time scale at ambient temperature. Isolation of the orange-red product in 95% yield followed by solution spectral analyses confirmed the formation of a complex with C_3 or averaged-C_3 symmetry. Specifically, a single $^{31}P\{^1H\}$ NMR signal at δ 22.10 and a single type of catecholate group in the ^1H and $^{13}C\{^1H\}$ NMR spectra were noted. In the proton spectrum, the H(3) catechol proton multiplet of the metallaligand moved dramatically downfield from δ 6.21 to 7.87 and became a broadened virtual triplet while the phenyl *ortho* protons also shifted slightly downfield from δ 7.28 to 7.63. All proton resonances were relatively broad, due probably to the onset of dynamic behavior.

In the proton-decoupled ^{13}C NMR spectrum of the product, the most significant observation is the appearance of virtual triplets (which were doublets in the $[TiL_3]^{2-}$ spectrum) in resonances for both catecholate and phenyl ring carbons. This strongly suggests a *trans*-phosphine coordination mode at the Pd^{II} centers.[69] Further, the catecholate C(4) resonance shifted upfield by over 5 ppm while a downfield coordination shift of 6 ppm is observed for C(3). Of the phenyl group carbons, similar significant coordination shifts were found for the *ipso* (−6.1 ppm) and *ortho* (+2.4 ppm) ring carbon resonances.

Positive ion FAB mass spectrometry in DMF (nitrobenzyl alcohol matrix) further confirmed the presence of $[Ti_2Pd_3Br_6L_6]^{4-}$ clusters with various counterion compositions (see Experimental Section). Other alkali metal salts of this cluster were prepared analogously from the corresponding $Li_2[TiL_3]$, $K_2[TiL_3]$, or $Rb_2[TiL_3]$ complexes. The $(DABCO\text{-}H)_4[Ti_2Pd_3Br_6L_6]$ cluster was prepared from $(DABCO\text{-}H)_2[TiL_3]$. Spectral data of these products are listed in the Experimental Section.

Similar assembly from the $Cs_2[SnL_3]$ precursor led to nearly quantitative formation of the $Cs_4[Sn_2Pd_3Br_6L_6]$ cluster. Finally, single-crystal X-ray diffraction studies of $Cs_4[Ti_2Pd_3Br_6L_6]$, $Cs_4[Sn_2Pd_3Br_6L_6]$ (cf. ref 36), and $(DABCO\text{-}H)_4[Sn_2Pd_3Br_6L_6]$ confirmed the structures of these clusters in the solid state (vide infra).

The use of DMF as a solvent was essential for clean formation of a single product. Less polar solvents such as methanol and acetonitrile yielded multiple products as well as insoluble material. Interestingly, attempts at cluster formation with several other cationic salts of $[TiL_3]^{2-}$ were unsuccessful. For example, tetraphenyl-phosphonium and PPN^+ salts of $[TiL_3]^{2-}$ yielded only insoluble material with $PdBr_2$ in all solvent systems attempted. In addition, both triethylammonium and tetramethylammonium precursors gave multiple products in DMF, as revealed by ^{31}P NMR spectroscopy (Figure 5a). A FAB-mass spectrum of the $[NEt_3H]_2$ $[TiL_3]/PdBr_2$ (2:3 mol ratio) reaction mixture in DMF gave no evidence of any cluster formation. However, addition of stoichiometric equivalents of cesium triflate to this solution resulted in formation of a single species whose NMR spectra and FAB mass spectrum confirmed the formation of $Cs_4[Ti_2Pd_3Br_6L_6]$ ($^{31}P\{^1H\}$ NMR spectrum, Figure 5b). Interestingly, the FAB mass spectrum revealed a propensity for the Cs^+ cations to be ionized with the cluster even when run in the positive mode (see Experimental Section). This suggests a strong interaction between the cluster and the Cs^+ cations even under these harsh conditions. In light of this and the solid-state structure of the complex discussed below, we suggest that the cesium cations remain embedded into the three cluster clefts even in solution, which may be essential for the integrity of the cluster. Fast exchange of these cluster-bound cesium cations with solvated cesium atoms was revealed by titrating 4 equiv of CsOTf into the cluster and observing the ^{133}Cs NMR spectra; only a single, averaged broad signal was observed at ambient temperature.

(63) We examined three possible factors that may favor the *fac*-isomer in solution. (1) *Sterics*: The remoteness of the three diphenylphosphino substituents from the metal center and from each other renders significant differences in *fac* versus *mer* steric strain energies unlikely. Molecular mechanics indeed showed very similar strain energies. Steric effect as the origin of any isomeric preference can be discounted. (2) *Electronic effect*: Electronically the PPh_2 group is known to be moderately electron withdrawing,[61,62] thus the existence of an intrinsic electronic effect (or *trans* influence) favoring the *fac*-isomer is feasible. However, DFT molecular orbital calculations (pBP-DN* with the Spartan 5.0 programs, Wavefunction, Inc.) on $[Ti(catecholato\text{-}4\text{-}PH_2)_3]^{2-}$ actually favored the *mer* over the *fac* as the ground-state configuration by 11.7 kJ/mol. Further, no convincing X-ray data consistent with differing metal−oxygen bond distances due to such a substituent effect have been found in either the $Sn(4\text{-}NO_2\text{-}catecholato)_3$ (*fac*) (Lamberth, C.; Machell, J. C.; Mingos, D. M. P.; Stolberg, T. L. *J. Mater. Chem.* **1991**, *1*, 775−780) or the Cs_2TiL_3 (*mer*) structure described above. (3) *Solvation effect*: Since the *fac*-isomer can be expected to have a substantially larger dipole moment than the *mer*-isomer (a substantially larger molecular dipole was found for the *fac*-isomer relative to the *mer*-isomer; 4.13 D versus 1.56 D from *PM3*(*tm*) calculations, and 1.2 D versus 0.54 D from DFT calculations). The resulting higher solvation energy in a polar solvent may be the origin of its predominance. In this case, a significant solvent polarity dependence of the speciation can be anticipated. Our NMR spectral data do show some solvent dependence. For example, both Li^+ and Cs^+ salts of TiL_3^{2-} showed broadened room temperature ^1H signals in CD_2Cl_2 compared to spectra in more polar CD_3OD or d_6-acetone. Interestingly, for TMA_2TiL_3, both the TMA as well as the ligand signals are broadened at room temperature in CD_2Cl_2 but not in CD_3OD or d_6-acetone. These observations, however, can be attributed just as well to differing ion pairing effects rather than to the emergence of a *mer*-isomer in a low polarity solvent. We therefore sought to remove the former influence by studying the PPN^+ salt of $[TiL_3]^{2-}$ since this bulky cation is not expected to participate in tight ion pairing. Both the ^1H and $^{31}P\{^1H\}$ NMR spectra of PPN_2TiL_3 in CD_2Cl_2 and d_6-acetone gave the sharp signals of a single C_3 solution species. Thus tight ion pairing is most likely the origin of the solvent-dependent spectra of the Li^+, Cs^+, and TMA^+ salts.

(64) Fay, R. C. *Coord. Chem. Rev.* **1996**, *154*, 99.

(65) Fay, R. C.; Lindmark, A. F. *J. Am. Chem. Soc.* **1983**, *105*, 2118.

(66) Wong, C. Y.; Woollins, J. D. C. C. R. *Coord. Chem. Rev.* **1994**, *130*, 175.

(67) Denekamp, C. I. F.; Evans, D. F.; Parr, J.; Woollins, J. D. *J. Chem. Soc., Dalton Trans.* **1993**, 1489.

(68) Woollins, J. D.; Parr, J. Personal communication.

(69) Pregosin, P. S.; Kunz, R. W.; Springer-Verlag: New York, 1979; p 89.

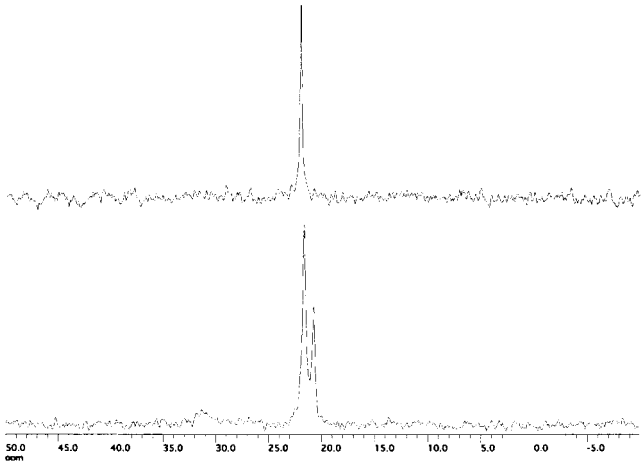

Figure 5. $^{31}P\{^1H\}$ NMR spectra of the reaction mixture of $[NEt_3H]_2$-Ti**L**$_3$ and $PdBr_2$·2PhCN (2:3 ratio) in DMF: (bottom) before and (top) after addition of 2 equiv of cesium triflate.

A 2:3 assembly of the C_3-M**L**$_3^{2-}$ and C_2-*trans*-$PdBr_2$ can yield either the D_3 helicate or the C_{3h} mesocate cluster. CAChe molecular modeling revealed that the latter should be considerably less sterically congested than the former.[47] The X-ray structural determinations of these clusters as described below indeed confirm the exclusive formation of mesocates in the solid state. Since the NMR data are consistent with the formation of a unique species, we conclude that this solid state mesocate structure is preserved in solution, although the possibility of a fast mesocate/helicate equilibration cannot be unequivocally discounted.

X-ray Structure of $Cs_4[Ti_2Pd_3Br_6L_6]$·9THF·H_2O·1.5Et_2O·1.5DMF. A single-crystal X-ray diffraction study confirmed the successful assembly of the desired heterometallic cluster. This has crystallographically imposed C_{3h} symmetry and is therefore a mesocate featuring one Ti center having Δ and the second the Λ configuration. The top and bottom Ti**L**$_3$ halves of the cluster are linked by three pseudo-square-planar $PdBr_2$ units, each *trans* coordinated by one PPh_2 group from each half (Figure 6). A 3-fold axis exists along the Ti···Ti axis with the metal centers separated by 6.76 Å. The twist angle around each Ti is 36.9°, almost halfway distorted from the octahedral twist angle of 60° toward the trigonal prismatic coordination geometry of 0° (Figure 7). While the average Ti-catecholato oxygen distance of 1.97 Å is normal, the Ti−O(1) distance of 1.949(5) Å is shorter than the Ti−O(2) distance of 1.984(5) Å. This may be a result of the strain imposed by formation of the cluster whereby *endo* Ti−O(2) bonds are stretched while *exo* Ti−O(1) bonds are compressed to accommodate the supramolecular structure. In accord with this, *exo* cluster O(1)−Ti−O(1′) angles are 88.3(2)° while *endo* O(2)−Ti−O(2′) are 89.2(2)°. Both O(1) and O(2) are also coordinated to Cs^+ cations.

Of particular interest is the location of the four cesium counterions. Three of these are deeply embedded in the three clefts of the cluster. Each symmetry equivalent Cs(2) is coordinated by four *endo*-catecholate oxygens in a rectangular array and two *exo*-THF solvent molecules which are buried in the clefts (Figure 6). The low coordination number (6) of these cesium cations results from the peripheral Br atoms from the three $PdBr_2$ moieties which, while not in van der Waals contact with the cations, effectively shield them from additional donors. Therefore, relatively short Cs−O distances are observed. Specifically, Cs(2) to catecholate O(2) has a distance of 3.138(5) Å while the 2.918(10) Å distance of Cs(2) to O(3) of a THF

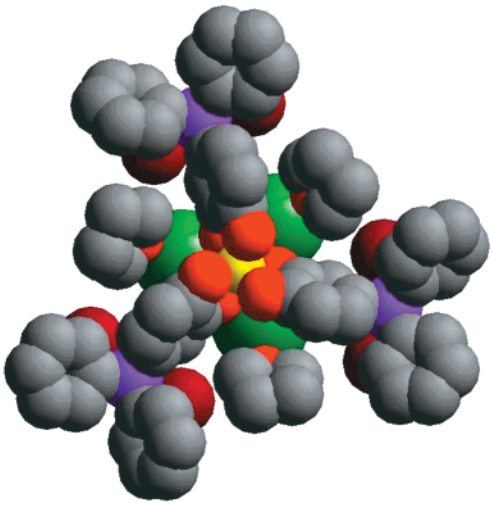

Figure 6. A view of the solid-state structure of $Cs_4[Ti_2L_6(PdBr_2)_3]$·6THF viewed down the crystallographic 3-fold axis of the cluster. One disordered Cs atom and all disordered solvent molecules and hydrogen atoms have been omitted for clarity. The purple spheres represent P atoms, brown spheres are Br atoms, green spheres are Cs atoms, yellow spheres are Ti atoms, gray spheres represent carbon, and red spheres are oxygen. The Pd ions are eclipsed by the coordinating phosphine ligands.

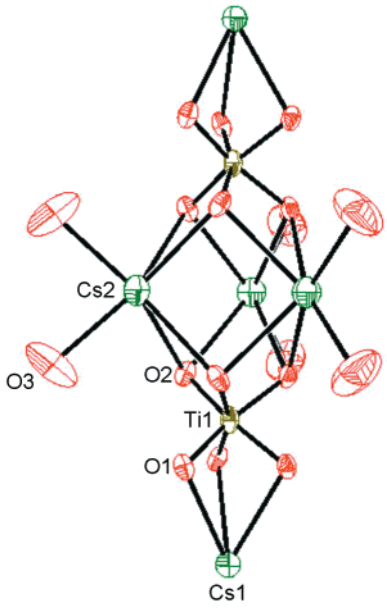

Figure 7. ORTEP view highlighting Ti and Cs coordination spheres in the solid-state structure of $Cs_4[Ti_2L_6(PdBr_2)_3]$. All carbon, nitrogen, phosphorus, palladium, bromine, and noncoordinating oxygen atoms are omitted for clarity. Thermal ellipsoids are at 50% probability.

is one of the shortest reported.[71] The three embedded cesium cations are separated from each other by 4.45 Å. The fourth Cs^+ is coordinated to the exterior of the anionic cluster and disordered equally over the two tris(catecholate)titanium cap oxygen sites (Figure 7). The Cs(1)−O(1) distance of 3.080(5) Å is again quite short. The remaining coordination sphere of this cesium is probably filled by disordered ether and DMF solvent molecules in the vicinity.

X-ray Structure of $Cs_4[Sn_2Pd_3Br_6L_6]$·3.5DMF·$2H_2O$·THF·*x*(solvent). Although the cluster has no crystallographically imposed symmetry, it is also a mesocate and has idealized C_{3h}

(70) Shannon, R. D. *Acta Crystallogr.* **1976**, *A 32*, 751.
(71) Allen, F. H.; Kennard, O. *Chem. Design Autom. News* **1993**, *8*, 31.

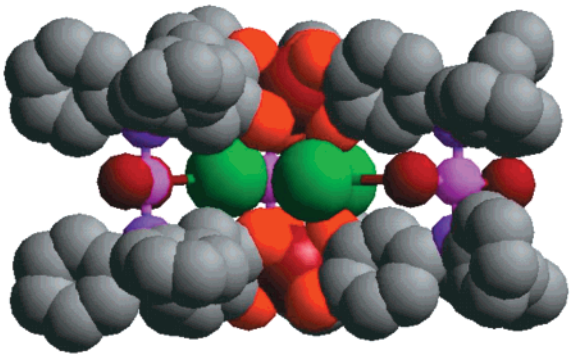

Figure 8. A view of the solid-state structure of $Cs_4[Sn_2\mathbf{L}_6(PdBr_2)_3]$ along the pseudomirror plane of the cluster. All disordered solvent molecules, all hydrogen atoms, and one of the disordered Cs atoms are omitted for clarity. The color scheme is the same as for Figure 6, with Sn atoms represented by brown spheres and Pd atoms as light purple spheres.

symmetry similar to the **$Cs_4[Ti_2Pd_3Br_6L_6]$** structure described above (Figure 8). Again, the two Sn atoms sit on an idealized 3-fold axis with a pseudomirror plane (through each of the three Pd atoms) linking the Δ- and Λ-tris(catecholate)tin halves via *trans* coordination of the PPh_2 groups. The Sn coordination spheres, with twist angles of 44.0° and 46.1°, are less distorted from octahedral than in the Ti analogue. The Sn···Sn separation is 6.88 Å, slightly longer than the Ti···Ti of 6.76 Å, presumably a result of the larger ionic radius of Sn^{IV} (0.830 Å) compared to Ti^{IV} (0.745 Å).[70]

Three of the four cesium cations (Cs(1), Cs(2), and Cs(3)) are well-ordered while a fourth is disordered over three sites (Cs(4), Cs(5), and Cs(6)). Both Cs(1) and Cs(3) are located in cluster clefts and are seven-coordinate. Cs(1) is coordinated by a rectangular array of *endo*-catecholate oxygens, two DMF molecules, and a bromide, Br(3), from a $PdBr_2$ moiety. Cs(3) is coordinated by four *endo*-catecholate oxygens, one DMF, and one water molecule, as well as a bromide, Br(5). Cs(2) sits atop Sn(2), slightly off the pseudo 3-fold axis, and is coordinated to three *exo*-catecholate oxygens, one DMF, and one water molecule (Figure 9). In addition, disordered solvent molecules probably complete its coordination sphere. The disordered fourth cesium cation is located with $^2/_3$ occupancy as Cs(4) in the third cluster cleft. The remaining $^1/_3$ occupancy is equally divided between two capping *exo* sites above Sn(1) at Cs(5) and Cs(6).

The palladium ions have a *pseudo*-square-planar geometry with normal Pd−P bond distances of 2.32−2.35 Å. An interesting feature of the structure is the deflection of one Br from each $PdBr_2$ linker toward the cluster cleft to coordinate the embedded Cs^+ cations (Figure 8). The larger intracluster Sn···Sn separation of 6.88 Å may facilitate this interaction. The average Cs−Br distance of 3.82 Å is well within the normal range of reported Cs−Br distances in the Cambridge Structural Database.[71] Other important bond distances and bond angles are listed in Table 3.

X-ray Structure of $(DABCO\text{-}H)_4[Sn_2Pd_3Br_6L_6]\cdot 3H_2O\cdot x$(solvent).[72] The core $Sn_2Pd_3\mathbf{L}_6$ cluster is again a C_{3h} mesocate as for the two structures discussed above (Figures 10 and 11). The twist angle around the tin center is 41.9° while the average Sn−O distance is 2.05 Å. Of interest is the significantly larger Sn···Sn separation of 7.47 Å compared to the 6.88 Å observed in the $Cs_4[Sn_2Pd_3\mathbf{L}_6]$ structure, presumably necessary for accommodating the three bulky DABCO groups within the cluster clefts.

(72) $(DABCO\text{-}H)_4[Sn_2Pd_3Br_6\mathbf{L}_6]\cdot 3H_2O\cdot x$(solvent): orange triangular prism, crystal size 0.42 × 0.06 × 0.06 mm³, FW = 3180.21, $T = -80$ °C, hexagonal space group, $P6_3/m$, $a = 23.2576(5)$ Å, $c = 16.7452(4)$ Å, $V = 7844.1(3)$ Å³, $Z = 2$, $R = 0.055$, $Rw = 0.078$, GOF = 2.47.

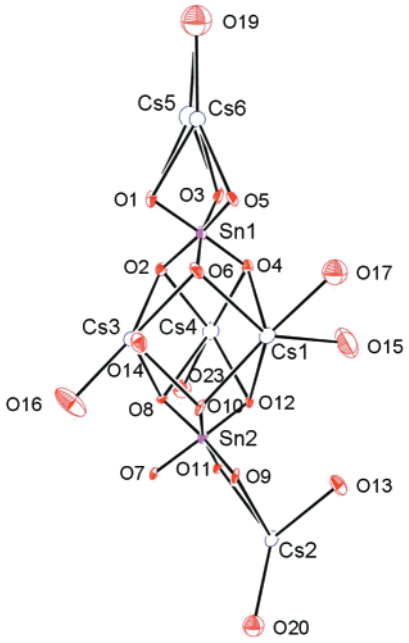

Figure 9. ORTEP view highlighting Sn and Cs coordination spheres in the solid-state structure of $Cs_4[Sn_2\mathbf{L}_6(PdBr_2)_3]$. All carbon, nitrogen, phosphorus, palladium, bromine, and noncoordinating oxygen atoms are omitted for clarity. Thermal ellipsoids are at 30% probability.

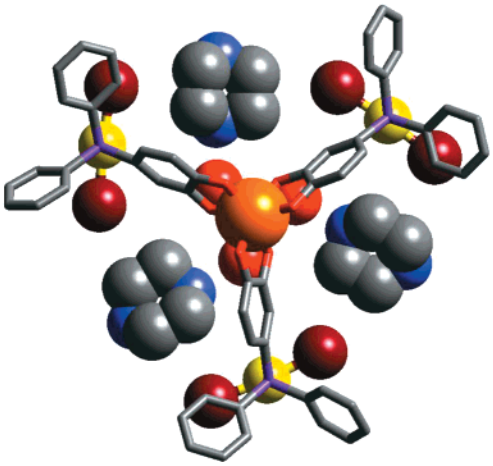

Figure 10. A view down the 3-fold axis of the solid-state structure of the $(DABCO\text{-}H)_4[Sn_2Pd_3Br_6\mathbf{L}_6]$ cluster. All disordered solvent molecules, all hydrogen atoms, and a DABCO-H have been omitted for clarity. The ligand is represented as a wireframe, Pd atoms are yellow spheres, Sn atoms are orange spheres, oxygen atoms of encapsulated solvent water molecules are represented as red spheres, Br atoms are brown spheres, and blue and gray spheres represent nitrogen and carbon atoms of the DABCO-H molecules, respectively.

Again, the three pseudo-square-planar palladium centers are *trans* coordinated by PPh_2 groups with a normal Pd−P bond length of 2.363(2) Å and nearly linear P−Pd−P angle of 174.5(1)°. While Br(1) sits 2.445(2) Å from the Pd center, the second Br is disordered over Br(2) and Br(3) sites 0.63 Å apart.

Three protonated DABCO cations sit in the expanded cluster clefts. In addition, three water molecules are sandwiched between the two Sn atoms and each is hydrogen bonded to two *endo*-catecholate oxygens as well as a protonated DABCO. A fourth protonated DABCO is not associated with the cluster and is treated as disordered *x*(solvent). Important bond distances and angles are presented in Table 4.

Figure 11. A stereoview of the solid-state structure of the (DABCO-H)$_4$[$Sn_2Pd_3Br_6$**L**$_6$] cluster along the mirror plane of the cluster. Again all disordered solvent molecules, all hydrogen atoms, and a DABCO-H have been omitted for clarity. All but the Sn ions, DABCO-H, and encapsulated solvent water molecules are shown as a wireframe. The same color scheme as in Figure 10 is used.

Table 2. Selected Bond Distances (Å) and Bond Angles (deg) for $Cs_4[Ti_2Pd_3Br_6L_6]$[a]

Cs(1)−O(1)	3.080(5)	O(1)−C(1)	1.340(8)
Cs(2)−O(3)	2.918(10)	O(2)−C(2)	1.344(8)
Cs(2)−O(2)	3.138(5)	O(3)−C(22)	1.28(2)
Cs(2)−O(2′)	3.181(5)	O(3)−C(19)	1.47(2)
Pd(1)−P(1)	2.326(2)	O(4)−C(26)	1.36(3)
Pd(1)−Br(2)	2.405(2)	O(4)−C(23)	1.58(2)
Pd(1)−Br(1)	2.4309(13)	Pd(1)−Br(3)	2.468(9)
Pd(1)−Br(4)	2.501(14)	Ti(1)−O(1)	1.949(5)
Ti(1)−O(2)	1.984(5)		
O(1)−Cs(1)−O(1′)	52.3(2)	O(3)−Cs(2)−O(3′)	83.9(6)
O(3)−Cs(2)−O(2)	91.4(3)	O(3)−Cs(2)−O(2′)	141.4(2)
P(1)−Pd(1)−P(1′)	178.17(10)	P(1)−Pd(1)−Br(2)	90.17(5)
P(1)−Pd(1)−Br(1)	90.12(5)	Br(2)−Pd(1)−Br(1)	161.9(2)
P(1)−Pd(1)−Br(3)	89.86(5)	Br(1)−Pd(1)−Br(3)	179.0(9)
P(1)−Pd(1)−Br(4)	89.67(5)	Br(1)−Pd(1)−Br(4)	166.7(9)
O(1)−Ti(1)−O(1′)	88.3(2)	O(1′)−Ti(1)−O(2)	105.7(2)
O(1)−Ti(1)−O(2)	80.0(2)	O(1′)−Ti(1)−O(2)	161.3(2)

[a] Primes represent symmetry equivalent atoms.

Summary of Solid-State Cluster Structures. All three clusters are mesocates featuring both enantiomeric forms of the C_3-symmetry M**L**$_3$ units linked by three *trans*-$PdBr_2$ bridges to give idealized C_{3h} symmetry in the solid state. The three deep molecular clefts of these clusters are occupied by the respective counterions of the tetranionic assembly. The larger Sn^{IV} (83 pm compared to 74.5 pm for Ti^{IV}) ionic radius and longer intracluster Sn···Sn separation (6.88 Å compared to 6.76 Å for Ti···Ti) enables an unusual deflection of the $PdBr_2$ units toward the embedded Cs^+ cations so that each coordinates to one bromide. To accommodate the even larger protonated DABCO cations, this Sn···Sn separation is increased to 7.47 Å, though these protonated tertiary amine cations are not directly coordinated to the *endo*-catecholate oxygens. Some disorder of the fourth cation as well as considerable disorder of the solvent molecules are noted in all three structures.

Syntheses of the [$M_2Pd_3X_6L_6$] (X = Cl, I) Clusters. Reaction of Cs_2Ti**L**$_3$ with $PdCl_2$·2PhCN (2:3 ratio) in DMF gave $Cs_4[Ti_2Pd_3Cl_6$**L**$_6]$ as a dark-red solid in 74% yield. Elemental and spectral analyses confirmed the formation of this cluster (see Experimental Section). The iodo analogue was prepared in quantitative yield by halide metathesis between $Cs_4[Ti_2Pd_3Br_6$**L**$_6]$ and CsI in DMF. Again both analytical and spectral data confirmed its formulation as $Cs_4[Ti_2Pd_3I_6$**L**$_6]$. A similar halide metathesis yielded $Cs_4[Sn_2Pd_3I_6$**L**$_6]$ from $Cs_4[Sn_2Pd_3Br_6$**L**$_6]$ and CsI. All these species exhibit the expected C_{3h} symmetry in solution based on NMR spectroscopy.

Syntheses of Other $M_2M'_3L_6$ Clusters. Extension of the *aufbau* assembly of the M_2Pd_3**L**$_6$ cluster motif with other C_2 linkers was attempted. Thus reaction of 3 equiv of *cis*-$Cr(CO)_4$(piperidine)$_2$ with 2 equiv of Cs_2Ti**L**$_3$ in DMF gave a cloudy orange solution after 5 days at room temperature. $^{31}P\{^1H\}$ NMR analysis revealed formation of a new complex with a resonance at δ +71.92 as well as the presence of unreacted Cs_2Ti**L**$_3$ at δ −4.74. In this case, the desired cluster $Cs_4[Ti_2\{Cr(CO)_4\}_3$**L**$_6]$ was successfully isolated after workup in 66% yield. Analogously, $Cs_4[Sn_2\{Cr(CO)_4\}_3$**L**$_6]$ was also synthesized in 74% yield and both have been characterized by elemental analyses, IR, and ^1H, $^{13}C\{^1H\}$, and $^{31}P\{^1H\}$ NMR spectroscopy. Compared to spectral data for *trans*-$Cr(CO)_4(PPh_3)_2$,[69] all these data are fully consistent with formation of the expected C_{3h} mesocate clusters featuring PPh_2-coordinated *trans*-$Cr(CO)_4$ linking groups. The single strong IR carbonyl stretching band at 1855 cm^{-1}

Table 3. Selected Bond Distances (Å) and Bond Angles (deg) for $Cs_4[Sn_2Pd_3Br_6L_6]$

Cs(1)−Br(3)	3.754(3)	Sn(1)−O(1)	2.05(2)
Cs(1)−O(4)	3.08(2)	Sn(1)−O(2)	2.08(2)
Cs(1)−O(6)	3.22(2)	Sn(1)−O(3)	2.06(2)
Cs(1)−O(10)	3.28(2)	Sn(1)−O(4)	2.07(2)
Cs(1)−O(12)	3.23(1)	Sn(1)−O(5)	2.06(2)
Cs(1)−O(15)	2.97(5)	Sn(1)−O(6)	2.04(2)
Cs(2)−O(9)	3.14(1)	Sn(2)−O(7)	2.06(2)
Cs(2)−O(11)	3.16(1)	Sn(2)−O(8)	2.07(2)
Cs(2)−O(11′)	3.18(2)	Sn(2)−O(9)	2.03(1)
Cs(2)−O(13)	3.07(2)	Sn(2)−O(10)	2.04(1)
Cs(2)−O(20)	3.14(5)	Sn(2)−O(11)	2.07(1)
Cs(3)−Br(5)	3.960(3)	Sn(2)−O(12)	2.08(2)
Cs(3)−O(2)	3.17(2)	Pd(1)−Br(1)	2.451(4)
Cs(3)−O(6)	3.25(2)	Pd(1)−Br(2)	2.424(4)
Cs(3)−O(8)	3.19(1)	Pd(1)−P(1)	2.331(7)
Cs(3)−O(10)	3.28(2)	Pd(1)−P(2)	2.345(6)
Cs(3)−O(16)	3.08(4)	Pd(2)−Br(3)	2.442(4)
Cs(4)−Br(1)	3.741(5)	Pd(2)−Br(4)	2.405(4)
Cs(4)−O(2)	3.27(2)	Pd(2)−P(3)	2.336(8)
Cs(4)−O(4)	3.27(1)	Pd(2)−P(4)	2.332(8)
Cs(4)−O(8)	3.21(2)	Pd(3)−Br(5)	2.446(2)
Cs(4)−O(12)	3.23(1)	Pd(3)−Br(6)	2.412(2)
Cs(4)−O(23)	2.90(4)	Pd(3)−P(5)	2.331(7)
Cs(5)−O(3)	2.96(2)	Pd(3)−P(6)	2.316(7)
Cs(5)−O(19)	3.31(8)	Cs(6)−O(1)	3.10(2)
Cs(6)−O(3)	3.05(2)	Cs(6)−O(5)	3.23(2)
Cs(6)−O(19)	3.30(8)		
Br(3)−Cs(1)−O(4)	138.5(2)	Br(3)−Cs(1)−O(6)	95.0(2)
Br(3)−Cs(1)−O(10)	89.9(2)	Br(3)−Cs(1)−O(12)	128.8(3)
Br(3)−Cs(1)−O(15)	103.8(7)	O(4)−Cs(1)−O(6)	55.3(4)
O(4)−Cs(1)−O(10)	115.0(4)	O(4)−Cs(1)−O(12)	92.1(3)
O(4)−Cs(1)−O(15)	89.3(8)	O(4)−Cs(1)−O(10)	89.4(5)
O(6)−Cs(1)−O(12)	115.4(4)	O(6)−Cs(1)−O(15)	140.6(8)
O(10)−Cs(1)−O(12)	52.8(4)	O(10)−Cs(1)−O(15)	124.4(7)
O(12)−Cs(1)−O(15)	78.8(7)		
O(1)−Sn(1)−O(2)	81.9(7)	O(1)−Sn(1)−O(3)	88.2(8)
O(1)−Sn(1)−O(4)	165.2(5)	O(1)−Sn(1)−O(5)	90.7(7)
O(1)−Sn(1)−O(6)	100.8(8)	O(2)−Sn(1)−O(3)	100.4(6)
O(2)−Sn(1)−O(4)	89.2(7)	O(2)−Sn(1)−O(5)	166.8(7)
O(2)−Sn(1)−O(6)	89.0(6)	O(3)−Sn(1)−O(4)	81.8(7)
O(3)−Sn(1)−O(5)	90.2(7)	O(3)−Sn(1)−O(6)	167.8(9)
O(4)−Sn(1)−O(5)	90.7(7)	O(4)−Sn(1)−O(6)	90.7(7)
O(5)−Sn(1)−O(6)	81.7(7)	O(7)−Sn(2)−O(8)	82.3(6)
O(7)−Sn(2)−O(9)	90.6(7)	O(7)−Sn(2)−O(10)	101.2(6)
O(7)−Sn(2)−O(11)	88.6(6)	O(7)−Sn(2)−O(12)	167.8(4)
O(8)−Sn(2)−O(9)	189.1(6)	O(8)−Sn(2)−O(10)	91.4(5)
O(8)−Sn(2)−O(11)	97.8(5)	O(8)−Sn(2)−O(12)	91.6(6)
O(9)−Sn(2)−O(10)	81.8(6)	O(9)−Sn(2)−O(11)	90.3(5)
O(9)−Sn(2)−O(12)	96.8(7)	O(10)−Sn(2)−O(11)	89.5(6)
O(10)−Sn(2)−O(12)	81.7(6)		
Br(1)−Pd(1)−Br(2)	172.4(1)	Br(1)−Pd(1)−P(1)	86.0(2)
Br(1)−Pd(1)−P(2)	87.7(2)	Br(2)−Pd(1)−P(1)	92.1(2)
Br(2)−Pd(1)−P(2)	93.6(2)	P(1)−Pd(1)−P(2)	172.7(2)
Br(3)−Pd(2)−Br(4)	162.9(2)	Br(3)−Pd(2)−P(3)	90.9(2)
Br(3)−Pd(2)−P(4)	91.7(2)	Br(4)−Pd(2)−P(3)	89.4(2)
Br(4)−Pd(2)−P(4)	89.9(2)	P(3)−Pd(2)−P(4)	173.4(3)
Br(5)−Pd(3)−Br(6)	174.4(2)	Br(5)−Pd(3)−P(5)	87.0(1)
Br(5)−Pd(3)−P(6)	87.4(1)	Br(6)−Pd(3)−P(5)	93.8(1)
Br(6)−Pd(3)−P(6)	91.2(1)	P(5)−Pd(3)−P(6)	171.5(3)
Cs(4)−Br(1)−Pd(1)	118.93(9)	Cs(1)−Br(3)−Pd(2)	123.8(1)
Cs(3)−Br(5)−Pd(3)	120.6(1)		

Table 4. Selected Bond Distances (Å) and Bond Angles (deg) for (H- DABCO)$_4$[$Sn_2Pd_3Br_6L_6$][a]

Sn(1)−O(1)	2.044(5)	O(1)−C(1)	1.332(8)
Sn(1)−O(2)	2.065(5)	O(2)−C(2)	1.371(8)
Pd(1)−Br(1)	2.445(2)	N(1)−C(19)	1.513(10)
Pd(1)−Br(2)	2.424(2)	N(1)−C(21)	1.49(2)
Pd(1)−Br(3)	2.393(2)	N(2)−C(20)	1.47(1)
Pd(1)−P(1)	2.363(2)	N(2)−C(22)	1.44(2)
O(1)−Sn(1)−O(1′)	89.7(2)	O(1)−Sn(1)−O(2)	80.4(2)
O(1)−Sn(1)−O(2′)	164.9(2)	O(1′)−Sn(1)−O(2)	101.6(2)
O(2)−Sn(1)−O(2′)	90.3(2)	P(1)−Pd(1)−Pd(1′)	174.5(1)
Br(1)−Pd(1)−Br(2)	173.7(1)	Br(1)−Pd(1)−Br(3)	171.3(5)
Br(1)−Pd(1)−P(1)	88.88(6)	Br(2)−Pd(1)−P(1)	91.39(6)
Br(3)−Pd(1)−P(1)	90.73(6)		

[a] Primes represent symmetry equivalent atoms generated by the crystallographic 3-fold axis.

Scheme 2

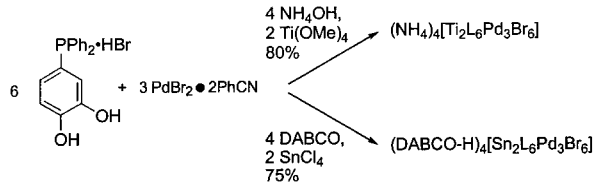

and the triplet carbonyl ^{13}C NMR resonance at δ +216 of the latter product support a local D_{4h} symmetry around the Cr centers.

To prepare a $Ga_2Pd_3\mathbf{L}_6$ cluster, 2 equiv of $Cs_3Ga\mathbf{L}_3$ and 3 equiv of $PdBr_2$·2PhCN were combined in DMF solvent yielding a clear, red solution that has a single ^{31}P{^{1}H} NMR resonance at δ +22. Both the ^{1}H and ^{13}C{^{1}H} NMR spectra also revealed the expected patterns, although the signals were severely broadened, indicative of significant dynamic behavior. Analytical data also supported a successful synthesis of the desired $Cs_3Ga_2(PdBr_2)_3\mathbf{L}_6$ cluster.

The Self-Assembly of $[M_2Pd_3Br_6L_6]^{4-}$ Clusters. The ultimate hybrid ligand should ideally exhibit sufficient discrimination between the two types of targeted incommensurate metal centers to allow a one-pot self-assembly of a single heterometallic cluster from a mixture of all the individual components. In our case, this requires the spontaneous assembly of 11 components (15, including the 4 equiv of base needed): 2 "C_3-symmetry" M^{IV} centers, 3 C_2 $PdBr_2$ units, as well as 6 equiv of ligand **L**. We have already noted the propensity of Pd^{II} to form very insoluble oligomeric material with $H_2\mathbf{L}$ under basic conditions (vide infra). We therefore sought alternative bases with higher solubility than the alkaline metal carbonates. Gratifyingly, successful self-assembly was achieved by using aqueous ammonia or DABCO solutions as the base in DMF solvent (Scheme 2). Both the $(NH_4)_4[Ti_2Pd_3Br_6\mathbf{L}_6]$[73] and (DABCO-H)$_4$[$Sn_2Pd_3Br_6\mathbf{L}_6$] clusters can be isolated in excellent yields via *spontaneous self-assembly* of the respective 11 components! The viability of this direct route broadens considerably the scope of cluster formation chemistry from our hybrid ligands.

Conclusion

The hybrid ligand 4-PPh_2-catechol combines a hard dianionic catecholate chelating site with a disparate soft phosphine donor group. The coordination of this ligand to metal centers with incommensurate symmetry requirements has led to novel supramolecular clusters through both stepwise *aufbau* synthesis and self-assembly routes to the variety of C_{3h} $M_2M'_3L_6$ clusters described herein. Extensions of this methodology to additional hard/soft metals as well as other ligand combinations promise to be an attractive and effective entry into other fascinating supramolecular assemblies. The *self-assembly* of these heterometallic clusters exemplifies our design strategy in which hard and soft chemical bonding preferences are satisfied while simultaneously forming a thermodynamically stable, discrete cluster.

Experimental Section

General Reaction Conditions and Reagent Sources. All operations and manipulations were performed in standard Schlenk glassware under a dry nitrogen atmosphere. Solvents were commercial reagent grade and degassed before use. The following reagents were prepared according to literature methods: 4-PCl_2-veratrole,[48] $PdBr_2$·2PhCN,[74] $PdCl_2$·2PhCN,[74] and $Cr(CO)_4$(piperidine)$_2$.[75]

Instrumentation and Methods. All NMR spectra were recorded on a Bruker AM 360 MHz or a JEOL FX-90Q spectrometer. Chemical shifts of ^{1}H and ^{13}C spectra are referenced to internal TMS. ^{31}P spectra were referenced to external 85% H_3PO_4. ^{119}Sn and ^{133}Cs NMR shifts were referenced to external $SnCl_4$ and CsCl, respectively. Electronic spectra were measured on a Cary 219 spectrophotometer and EPR spectra on a Varian E-4 instrument. Infrared spectra were run on a Nicolet MX-1 FT-spectrophotometer with use of KBr pellets. Elemental analyses were performed by the UNH Instrumentation Center on a Perkin-Elmer 2400 Elemental Analyzer. FAB mass spectra were run in an NBA matrix and carried out at the UC-Berkeley Mass Spectrometry Facility. Single-crystal X-ray diffraction data were collected on a Siemens SMART diffractometer in the Chexray facility at UC-Berkeley.

4-Diphenylphosphino-Veratrole (4-PPh_2-Veratrole). A three-neck flask under nitrogen was charged with magnesium (3.5 g, 0.14 mol) and dry diethyl ether (80 mL) and chilled to 0 °C in an ice bath. A solution of bromobenzene (14 mL, 0.13 mol) in 40 mL of dry diethyl ether was added to the flask dropwise while the mixture in the flask was stirred. After addition the mixture was heated to reflux for 1 h, and then cooled to 0 °C. A solution of 4-dichlorophosphino-veratrole (7.8 g, 33 mmol) in 30 mL of dry diethyl ether was added dropwise to the vigorously stirring mixture. Upon addition a white precipitate was produced. This mixture was heated to reflux again for 2 h, then cooled to 0 °C. Water (50 mL) was added dropwise to quench the excess Grignard reagent (*CAUTION!* The first few drops caused a rigorous reaction producing plenty of heat). The mixture was then filtered in air, and the filtrate was reduced by rotary evaporation and dried in a vacuum to yield 10.2 g of a yellowish-white solid. Recrystallization of this solid from ethanol (25 mL) afforded a pure white solid. Yield: 9.5 g, 29 mmol (88%).

^{1}H NMR (360 MHz, $CDCl_3$): δ 7.33 (m, 10 phenyl-H), 6.89 (m, 3-cat-H), 3.90 (s, $-OCH_3$), 3.77 (s, OCH_3). ^{13}C {^{1}H} NMR (89.9 MHz, $CDCl_3$): δ 149.8 (s, veratrole), 149.0 (d, J_{pc} = 10.0 Hz, veratrole), 137.6 (broad, phenyl), 133.5 (d, J_{pc} = 18.6 Hz, phenyl), 128.6 (s, phenyl), 128.5 (d, J_{pc} = 6.6 Hz, phenyl), 127.9 (broad, veratrole), 127.2 (d, J_{pc} = 19.4 Hz, veratrole), 116.6 (d, J_{pc} = 25.2 Hz, veratrole), 111.3 (d, J_{pc} = 8.0 Hz, veratrole), 55.8 (s, OCH_3). ^{31}P {^{1}H} NMR (36.3 MHz, $CDCl_3$): δ −5.35 (s). IR (KBr) $\upsilon_{(OCH3)}$ 2957, 2833 cm^{-1}, C−H bending 1507, 1438 cm^{-1}, $\upsilon_{(C-O-C)}$ 1254, 1235 cm^{-1}. Anal. Calcd for $C_{20}H_{19}PO_2$: C, 74.52; H, 5.94. Found: C, 74.31; H, 5.71.

4-Diphenylphosphino-Catechol, Hydrobromide Salt, 4-PPh_2-catechol·HBr (H_2L·HBr). A mixture of 4-diphenylphosphino-veratrole (5.0 g, 16 mmol) and 32 mL of 48% aqueous hydrobromic acid (0.28 mol) was refluxed under nitrogen for 18 h. Upon chilling, 4.7 g (13 mmol) of product precipitated. Recrystallization of this solid from ethanol (20 mL) and 48% aqueous hydrobromic acid (2 mL) provided a white solid. Yield: 4.1 g, 11 mmol (70%). ^{1}H NMR (360 MHz, DMF-d_7): δ 7.40 (m, 6 phenyl-H), 7.28 (m, 4 phenyl-H), 6.93 (dd, J = 7.9 and 1.53 Hz, 1 cat-H), 6.82 (dd, J = 7.53 and 1.73 Hz, 1 cat-H), 6.71 (ddd, J = 8.23, 8.23, and 1.53 Hz, 1 cat-H). ^{13}C{^{1}H} NMR (89.9 MHz, DMF-d_7): δ 147.6 (s, catechol), 146.5 (d, J_{pc} = 8.6 Hz, catechol), 138.8

(73) A preliminary single-crystal X-ray structure has confirmed the existence of this mesocate in the solid state: Sun, X.; Johnson, D. W.; Clarke, K. M.; Raymond, K. N.; Wong, E. H. Unpublished results.

(74) Anderson, G. K.; Lin, M. *Inorg. Synth.* **1990**, *28*, 61.

(75) Atwood, J. L.; Darensbourg, D. J. *Inorg. Chem.* **1977**, *16*, 2314.

(d, J_{pc} = 11.3 Hz, phenyl), 133.4 (d, J_{pc} = 19.2 Hz, phenyl), 128.9 (s, phenyl), 128.8 (d, J_{pc} = 3.3 Hz, phenyl), 126.3 (d, J_{pc} = 25.2 Hz, catechol), 125.9 (d, J_{pc} = 7.3 Hz, catechol), 121.4 (d, J_{pc} = 18.5 Hz, catechol), 116.5 (d, J_{pc} = 10.0 Hz, catechol); $^{31}P\{^1H\}$ NMR (36.3 MHz, DMF-d_7): δ −6.73 (s). IR (KBr) $\upsilon_{(OH)}$ broad 3290 cm^{-1}, $\upsilon_{(aromatic-H)}$ 3077, 3049, 3029 cm^{-1}, C−H bending 1509, 1439 cm^{-1}, $\upsilon_{(C-OH)}$ 1291, 1266 cm^{-1}. Anal. Calcd for $C_{18}H_{16}PO_2Br$: C, 57.62; H, 4.30. Found: C, 57.37; H, 4.38.

Cs_3[(4-PPh_2-Catecholato)$_3$Ga] (Cs_3[GaL_3]). A mixture of $Ga(NO_3)_3\cdot 6H_2O$ (264 mg, 0.731 mmol), 4-PPh_2-Catechol·HBr (815 mg, 2.17 mmol), and Cs_2CO_3 (1063 mg, 3.26 mmol) was stirred in 30 mL of degassed methanol under nitrogen atmosphere at room temperature for 3 days, giving a slightly cloudy solution. The solution was filtered through a frit with Celite and glasswool (pre-purged by nitrogen) under nitrogen to give a colorless clear filtrate, which was then evaporated in a vacuum to give a white powder. The white solid was washed with degassed water three times, and dried overnight in a vacuum. Yield: 842 mg (86%). ^1H NMR (360 MHz, d_4-methanol): δ 7.24 (m, 3 × 10 phenyl-H), 6.51 (m, 3 × 3 cat-H). ^1H NMR (360 MHz, d_7-DMF): δ 7.29 (m, 3 × 10 phenyl-H), 6.46 (broad d, J = 8.5 Hz, 3 × 1 cat-H), 6.38 (broad d, J = 6.7 Hz, 3 × 1 cat-H), 6.27 (broad t, J = 8.5 Hz, 3 × 1 cat-H). $^{13}C\{^1H\}$ NMR (89.9 MHz, d_4-methanol): δ 158.0 (s, catechol), 156.5 (d, J_{pc} = 10.0 Hz, catechol), 141.5 (d, J_{pc} = 10.0 Hz, phenyl), 134.3 (d, J_{pc} = 18.5 Hz, phenyl), 129.2 (d, J_{pc} = 6.3 Hz, phenyl), 129.0 (s, phenyl), 125.2 (d, J_{pc} = 27.4 Hz, catechol), 120.6 (s, catechol), 119.0 (d, J_{pc} = 18.4 Hz, catechol), 113.9 (d, J_{pc} = 12.4 Hz, catechol). $^{31}P\{^1H\}$ NMR (36.3 MHz, d_4-methanol) δ −6.02 (s). Elemental Anal. Calcd for $Cs_3GaC_{54}H_{39}P_3O_6$: C, 48.21; H, 2.92. Found: C, 48.25; H, 3.02.

Cs_3[(4-PPh_2-Catecholato)$_3$Fe] (Cs_3[FeL_3]). A mixture of $Fe(NO_3)_3\cdot 9H_2O$ (135 mg, 0.333 mmol), 4-PPh_2-Catechol·HBr (375 mg, 1.00 mmol), and Cs_2CO_3 (490 mg, 1.50 mmol) was stirred in 20 mL of degassed methanol under a nitrogen atmosphere at room temperature for 4 days, giving a dark purple-red mixture. The mixture was filtered through a frit under nitrogen, and the blood-red filtrate was then evaporated in vacuo to give a dark-red residue. Acetone (3 × 10 mL) was used to extract the product. Evaporation of the dark-red acetone solution in vacuo gave a dark-red solid. Yield: 112 mg (25%). No NMR spectrum for this product is available due to the paramagnetism of iron^{III}. EPR spectrum (1.0 mM in methanol): g = 8.18, 4.25, 2.34. UV/vis spectrum (methanol solution): λ_{max} 323 nm (ϵ = 31 905), λ_{max} 490 nm (ϵ = 6050). IR (KBr): C−H bending 1474 cm^{-1}, $\upsilon_{(C-O-Fe)}$ 1254 cm^{-1}. Anal. Calcd for $Cs_3FeC_{54}H_{39}P_3O_6$: C, 48.72; H, 2.95. Found: C, 48.78; H, 2.94.

Alkali Metal Salts of [(4-PPh_2-Catecholato)$_3$Ti]$^{2-}$ ([TiL_3]$^{2-}$). The respective alkali metal carbonate was used in each preparation. The following procedure for **Cs_2[(4-PPh_2-Catecholato)$_3$Ti]** was followed**:** A mixture of $Ti(OMe)_4$ (387 mg, 2.14 mmol), 4-PPh_2-Catechol·HBr (2420 mg, 6.44 mmol), and Cs_2CO_3 (1760 mg, 5.40 mmol) was stirred in 60 mL of degassed methanol under nitrogen atmosphere at room temperature for 42 h, giving an orange-red suspension. The suspension was filtered through a frit under nitrogen to give an orange-red solid, which was then washed with degassed water at least three times and dried under vacuum overnight. The product (ca.. 2.0 g) was obtained in yields of around 78%. ^1H NMR (360 MHz, d_6-acetone): δ 7.25 (m, 3 × 10 phenyl-H), 6.53 (ddd, J = 9.6, 7.9 and 1.8 Hz, 3 × 1 cat-H), 6.39 (dd, J = 8.1 and 1.8 Hz, 3 × 1 cat-H), 6.35 (dd, J = 7.8 and 1.5 Hz, 3 × 1 cat-H). $^{13}C\{^1H\}$ NMR (89.9 MHz, d_6-acetone): δ 162.5 (s, catechol), 161.8 (d, J_{pc} = 11.0 Hz, catechol), 140.8 (d, J_{pc} = 12.5 Hz, phenyl), 133.9 (d, J_{pc} = 18.8 Hz, phenyl), 129.0 (d, J_{pc} = 6.3 Hz, phenyl), 128.7 (s, phenyl), 125.9 (d, J_{pc} = 23.8 Hz, catechol), 122.7 (d, J_{pc} = 3.8 Hz, catechol), 117.2 (d, J_{pc} = 21.9 Hz, catechol), 112.3 (d, J_{pc} = 10.9 Hz, catechol). $^{31}P\{^1H\}$ NMR (36.3 MHz, d_6-acetone) δ −4.88 (s). IR (KBr): $\upsilon_{(aromatic-H)}$ 3051, 3009, 1468 cm^{-1}, $\upsilon_{(C-O-Ti)}$ 1248 cm^{-1}. Elemental Anal. Calcd for $Cs_2TiC_{54}H_{39}P_3O_6$: C, 54.50; H, 3.30. Found: C, 54.46; H, 3.24.

(DABCO-H)$_2$[(4-PPh_2-Catecholato)$_3$Ti] ((DABCO·H)$_2$[TiL_3]). A mixture of $Ti(OMe)_4$ (100 mg, 0.550 mmol), 4-PPh_2-Catechol·HBr (626 mg, 1.67 mmol), and DABCO (3.0 g, in excess of 10 equiv) was stirred in 20 mL of degassed methanol under nitrogen atmosphere at room temperature for 3 days, giving an orange-red suspension. It was concentrated to half volume under vacuum and filtered through a frit under nitrogen atmosphere to give an orange-red residue. This solid was then washed with degassed water three times and dried in a vacuum overnight. An orange-red solid (460 mg) was obtained in a yield of 73%. ^1H NMR (360 MHz, d_7-DMF): δ 7.30 (m, 3 × 10 phenyl-H), 6.55 (ddd, J = 10.0, 7.7 and 1.8 Hz, 3 × 1 cat-H), 6.26 (dd, J = 7.7 and 1.6 Hz, 3 × 1 cat-H), 6.12 (dd, J = 7.3 and 1.7 Hz, 3 × 1 cat-H), 3.22 (s, 2 × 12 DABCO-H). $^{13}C\{^1H\}$ NMR (89.9 MHz, d_7-DMF): δ 162.2 (s, catechol), 160.6 (d, J_{pc} = 8.0 Hz, catechol), 140.2 (d, J_{pc} = 12.5 Hz, phenyl), 133.3 (d, J_{pc} = 18.7 Hz, phenyl), 128.6 (d, J_{pc} = 6.2 Hz, phenyl), 128.3 (s, phenyl), 125.5 (d, J_{pc} = 31.6 Hz, catechol), 121.6 (d, J_{pc} = 4.7 Hz, catechol), 115.9 (d, J_{pc} = 14.1 Hz, catechol), 111.2 (d, J_{pc} = 13.2 Hz, catechol), 45.1 (s). $^{31}P\{^1H\}$ NMR (36.3 MHz, DMF/d_6-benzene) δ −5.35 (s). IR (KBr): $\upsilon_{(N-H)}$ 3431 cm^{-1}, $\upsilon_{(aromatic\ C-H)}$ 3051, 3010 cm^{-1}, $\upsilon_{(-CH2CH2-)}$ 2961, 2952, 2884 cm^{-1}, C−H bending 1469 cm^{-1}, $\upsilon_{(C-O-Ti)}$ 1249 cm^{-1}. Elemental Anal. Calcd for $TiN_4C_{66}H_{65}P_3O_6$: C, 68.87; H, 5.69; N, 4.87. Found: C, 68.74; H, 5.90; N, 4.68.

Cs_2[(4-PPh_2-Catecholato)$_3$Sn] (Cs_2[SnL_3]). To a colorless solution of $SnCl_4$ (295 mg, 1.13 mmol) in degassed methanol (40 mL) under nitrogen were added 4-PPh_2-catechol·HBr (1.27 g, 3.40 mmol) and Cs_2CO_3 (1.66 g, 5.10 mmol). (CAUTION! The first few drops of methanol must be added slowly to avoid $SnCl_4$ boiling over due to the rigorous methanolysis of $SnCl_4$.) The mixture was stirred under a nitrogen atmosphere at room temperature for 3 days giving a white suspension. This was concentrated to half volume under vacuum and filtered through a frit under a nitrogen atmosphere to give a white solid. The solid was then washed with degassed water three times, and dried in vacuo overnight to yield white solid. This solid was recrystallized from acetone/diethyl ether. Yield: 898 mg, 62%. ^1H NMR (360 MHz, d_6-acetone): δ 7.27 (m, 3 × 10 phenyl-H), 6.63 (dd, J = 8.7 and 1.5 Hz, 3 × 1 cat-H), 6.56 (dd, J = 7.7 and 1.6 Hz, 3 × 1 cat-H), 6.40 (dd, J = 9.4, 7.8 and 1.9 Hz, 3 × 1 cat-H). $^{13}C\{^1H\}$ NMR (89.9 MHz, d_6-acetone): δ 154.9 (s, catechol), 153.5 (d, J_{pc} = 10.6 Hz, catechol), 141.0 (d, J_{pc} = 12.5 Hz, phenyl), 134.0 (d, J_{pc} = 18.7 Hz, phenyl), 129.0 (d, J_{pc} = 6.1 Hz, phenyl), 128.7 (s, phenyl), 124.7 (d, J_{pc} = 24.3 Hz, catechol), 121.5 (d, J_{pc} = 4.0 Hz, catechol), 119.5 (d, J_{pc} = 21.6 Hz, catechol), 114.4 (d, J_{pc} = 10.9 Hz, catechol). $^{31}P\{^1H\}$ NMR (36.3 MHz, d_6-acetone): δ −4.04 (s). IR (KBr): $\upsilon_{(aromatic\ C-H)}$ 3051, 3002 cm^{-1}, C−H bending 1473 cm^{-1}, $\upsilon_{(C-O-Ti)}$ 1246 cm^{-1}. Elemental Anal. Calcd for $Cs_2SnC_{54}H_{39}P_3O_6$: C, 51.42; H, 3.12. Found: C, 51.32; H, 3.16.

Cs_4[$Ti_2L_6Pd_3Br_6$]. A mixture of Cs_2[Ti**L**$_3$] (416 mg, 0.350 mmol) and $PdBr_2\cdot 2PhCN$ (248 mg, 0.525 mmol) was stirred in 20 mL of DMF under a nitrogen atmosphere at room temperature for 2 h giving a clear orange solution. Addition of 200 mL of THF precipitated an orange-yellow solid, which was filtered off and dried under vacuum. Yield: 526 mg (95%). Redissolving about 50 mg of this product in a mixed solvent of DMF/THF (v/v 1/5, 10 mL) gave a clear orange-red solution. Slow diffusion of diethyl ether into this solution gave well-formed X-ray quality orange-red crystals. ^1H NMR (360 MHz, d_7-DMF): δ 7.89 (t, J = 6.4 Hz, 6 × 1 cat-H), 7.63 (broad, 6 × 4 phenyl-H), 7.37 (broad, 6 × 6 phenyl-H), 6.40 (broad, 6 × 1 cat-H), 6.25 (broad d, J = 7.9 Hz, 6 × 1 cat-H). $^{13}C\{^1H\}$ NMR (89.9 MHz, d_7-DMF): δ 163.8 (s, catechol), 159.9 (virtual t, J_{PC} = 10.3 Hz, catechol), 134.7 (virtual t, J_{PC} = 5.6 Hz, phenyl), 134.4 (virtual t, J_{PC} = 20.2 Hz, phenyl), 129.7 (s, phenyl), 127.6 (virtual t, J_{PC} = 5.0 Hz, phenyl), 125.0 (s, catechol), 121.9 (virtual t, J_{PC} = 13.9 Hz, catechol), 115.7 (virtual t, J_{PC} = 28.2 Hz, catechol), 111.0 (virtual t, J_{PC} = 6.0 Hz, catechol). $^{31}P\{^1H\}$ NMR (36.3 MHz, d_7-DMF) δ 22.10 (s). IR (KBr): C−H bending 1474 cm^{-1}, $\upsilon_{(C-O-Ti)}$ 1258 cm^{-1}. Anal. Calcd for $Cs_4Ti_2C_{108}H_{78}P_6O_{12}Pd_3Br_6$: C, 40.80; H, 2.47. Found: C, 40.65; H, 2.41. FAB$^+$ MS m/z (nitrobenzyl alcohol matrix in DMF) (▲ = $[Ti_2L_6Pd_3]^{2+}$) {species, observed m/z (calculated m/z)}: [▲ + $6Br^-$ + $5Cs^+$]$^{1+}$, 3311 (3312.6); [▲ + $6Br^-$+ $4Cs^+$ + $1H^+$]$^{1+}$, 3179 (3180.7); [▲ + $6Br^-$+ $3Cs^+$ + $2H^+$]$^{1+}$, 3049 (3048.8); [▲ + $5Br^-$+ $3Cs^+$ + $1H^+$]$^{1+}$, 2968 (2967.9); [▲ + $4Br^-$ + $3Cs^+$]$^{1+}$, 2886 (2887.0); [▲ + $5Br^-$+ $2Cs^+$ + $2H^+$]$^{1+}$, 2835 (2836.0); [▲ + $6Br^-$+ $1Cs^+$ + $3H^{+-}$+ $1Na^+$]$^{1+}$, 2807 (2807.0); [▲ + $4Br^-$+ $2Cs^+$ + $1H^+$]$^{1+}$, 2755 (2755.1); [▲ + $6Br^-$ + $4H^{+-}$+ $1Na^+$]$^{1+}$, 2675 (2675.1).

$Cs_4[Sn_2L_6Pd_3Br_6]$. A DMF (15 mL) solution of $Cs_2[SnL_3]$ (233 mg, 0.176 mmol) and $PdBr_2$·2PhCN (124 mg, 0.263 mmol) was stirred under a nitrogen atmosphere at room temperature for 2 h giving a dark-red solution. Addition of 200 mL of THF precipitated an orange-yellow solid, which was filtered off and dried in a vacuum. Yield: 270 mg (89%). Redissolving about 50 mg of the product in 10 mL of DMF gave a clear orange-red solution. Slow diffusion of diethyl ether into this solution gave well-formed orange-red crystals of X-ray quality. ^{1}H NMR (360 MHz, d_7-DMF): δ 8.15 (broad, 6 × 1 cat-H), 7.66 (broad, 6 × 4 phenyl-H), 7.39 (broad, 6 × 6 phenyl-H), 6.57 (bd, J = 7.6 Hz, 6 × 1 cat-H), 6.25 (broad, 6 × 1 cat-H). ^{13}C{^{1}H} NMR (89.9 MHz, d_7-DMF): δ 156.2 (s, catechol), 151.5 (virtual t, J_{PC} = 10.0 Hz, catechol), 134.9 (virtual t, J_{PC} = 5.6 Hz, phenyl), 134.2 (virtual t, J_{PC} = 24.8 Hz, phenyl), 129.8 (s, phenyl), 127.6 (virtual t, J_{PC} = 5.0 Hz, phenyl), 123.8 (s, catechol), 120.6 (virtual t, J_{PC} = 13.4 Hz, catechol), 114.7 (virtual t, J_{PC} = 28.2 Hz, catechol), 113.4 (virtual t, J_{PC} = 4.0 Hz, catechol). ^{31}P{^{1}H} NMR (36.3 MHz, d_7-DMF): δ 21.61 (s). IR (KBr): C−H bending 1479 cm^{-1}, $\upsilon_{(C-O-Sn)}$ 1254 cm^{-1}. Elemental Anal. Calcd for $Cs_4Sn_2C_{108}H_{78}P_6O_{12}Pd_3Br_6$: C, 39.05; H, 2.37. Found: C, 38.91; H, 2.29.

(DABCO-H)$_4$[$Sn_2L_6Pd_3Br_6$]. (a) ***Aufbau Route.*** A DMF (20 mL) solution of (DABCO-H)$_2$[Sn**L**$_3$] (424 mg, 0.350 mmol) and $PdBr_2$·2PhCN (248 mg, 0.525 mmol) was stirred under nitrogen atmosphere at room temperature. Initial turbidity disappeared to give a dark-red solution in 4 h. Addition of 200 mL of THF precipitated an orange-yellow solid, which was filtered off and dried under vacuum. Yield: 390 mg (69%).

(b) ***Self-Assembly Approach.*** A suspension of $SnCl_4$, PPh_2-Catechol·HBr, $PdBr_2$·2PhCN, and DABCO in a molar ratio of 2:6:3:18 was stirred in degassed DMF under a nitrogen atmosphere at room temperature for a week giving a dark-red cloudy solution. This was filtered through a frit with Celite and glasswool to give a dark-red filtrate. The filtrate was evaporated in vacuo to give a dark-red solid in over 75% yield. Redissolving ca. 20 mg of the product in 5 mL of DMF gave a clear orange-red solution. Slow diffusion of diethyl ether into this solution gave well-formed orange-red crystals of X-ray quality.^{1}H NMR (360 MHz, d_7-DMF): δ 9.98 (flat, 4 × N−H), 8.31 (dd, J = 7.6 and 1.8 Hz, 6 × 1 cat-H), 7.58 (broad, 6 × 4 phenyl-H), 7.35 (broad, 6 × 6 phenyl-H), 6.74 (dt, J = 8.2 and 1.6 Hz, 6 × 1 cat-H), 6.50 (broad m, 6 × 1 cat-H), 3.16 (s, 4 × 12 DABCO-H). ^{13}C{^{1}H} NMR (89.9 MHz, d_7-DMF): δ 157.0 (s, catechol), 152.1 (virtual t, J_{PC} = 10.0 Hz, catechol), 134.8 (virtual t, J_{PC} = 25.9 Hz, phenyl), 134.6 (virtual t, J_{PC} = 5.3 Hz, phenyl), 129.6 (s, phenyl), 127.4 (virtual t, J_{PC} = 5.0 Hz, phenyl), 125.6 (virtual t, J_{PC} = 2.3 Hz, catechol), 124.5 (virtual t, J_{PC} = 13.9 Hz, catechol), 113.9 (virtual t, J_{PC} = 4.2 Hz, catechol), 112.6 (virtual t, J_{PC} = 27.2 Hz, catechol), 45.3 (s, DABCO). ^{31}P{^{1}H} NMR (36.3 MHz, d_7-DMF): δ 20.73 (s). IR (KBr): $\upsilon_{(N-H)}$ 3425 cm^{-1}, $\upsilon_{(aromatic\ C-H)}$ 3051, 3006 cm^{-1}, $\upsilon_{(-CH_2CH_2-)}$ 2952, 2883 cm^{-1}, C−H bending 1478 cm^{-1}, $\upsilon_{(C-O-Sn)}$ 1253 cm^{-1}. Anal. Calcd for $C_{132}H_{130}P_6O_{12}N_8Sn_2Pd_3Br_6$: C, 48.90; H, 4.04; N, 3.46. Found: C, 48.83; H, 3.96; N, 3.49.

$Cs_4[Ti_2L_6Pd_3Cl_6]$. A DMF (10 mL) solution of $Cs_2[TiL_3]$ (208 mg, 0.175 mmol) and $PdCl_2$·2PhCN (100 mg, 0.261 mmol) was stirred under a nitrogen atmosphere at room temperature for 2 h giving a clear dark-red solution. Addition of 100 mL of diethyl ether precipitated a dark-red solid that was filtered off and dried in vacuo. Yield: 220 mg (74%). ^{1}H NMR (360 MHz, d_7-DMF): δ 7.86 (broad t, J = 7.2 Hz, 6 × 1 cat-H), 7.63 (broad m, 6 × 4 phenyl-H), 7.40 (broad m, 6 × 6 phenyl-H), 6.32 (broad, 6 × 1 cat-H), 6.23 (broad m, 6 × 1 cat-H). ^{13}C{^{1}H} NMR (89.9 MHz, d_7-DMF): δ 163.9 (s, catechol), 159.8 (virtual t, J_{PC} = 10.0 Hz, catechol), 134.8 (virtual t, J_{PC} = 6.0 Hz, phenyl), 132.8 (virtual t, J_{PC} = 24.6 Hz, phenyl), 130.0 (s, phenyl), 127.8 (virtual t, J_{PC} = 5.0 Hz, phenyl), 124.6 (s, catechol), 121.0 (m, catechol), 114.6 (virtual t, J_{PC} = 27.9 Hz, catechol), 111.2 (m, catechol). ^{31}P{^{1}H} NMR (36.3 MHz, d_7-DMF): δ 24.03 (s). IR (KBr): C−H bending 1475 cm^{-1}, $\upsilon_{(C-O-Ti)}$ 1264 cm^{-1}. Anal. Calcd for $Cs_4Ti_2C_{108}H_{78}P_6O_{12}Pd_3Cl_6$: C, 44.53; H, 2.70. Found: C, 44.25; H, 2.51.

$Cs_4[Ti_2L_6Pd_3I_6]$. Addition of CsI (491 mg, 1.89 mmol) to 20 mL of DMF solution of $Cs_4[Ti_2L_6Pd_3Br_6]$ (200 mg, 0.0629 mmol) resulted in a cloudy mixture, which was stirred overnight. The mixture was filtered through a frit with Celite and glasswool, giving a dark-red filtrate that was evaporated in a vacuum to give a dark-red solid. Yield: 212 mg (97%). Redissolving about 30 mg of the product in 10 mL of DMF gave a clear dark-red solution. Slow diffusion of diethyl ether into this solution gave well-formed dark-red crystals. ^{1}H NMR (360 MHz, d_7-DMF): δ 7.78 (broad t, J = 7.3 Hz, 6 × 1 cat-H), 7.65 (broad m, 6 × 4 phenyl-H), 7.38 (broad, 6 × 6 phenyl-H), 6.55 (broad m, 6 × 1 cat-H), 6.32 (broad d, J = 7.9 Hz, 6 × 1 cat-H). ^{13}C{^{1}H} NMR (89.9 MHz, d_7-DMF): δ 162.9 (s, catechol), 158.0 (virtual t, J_{PC} = 10.0 Hz, catechol), 136.3 (virtual t, J_{PC} = 25.2 Hz, phenyl), 134.2 (virtual t, J_{PC} = 5.6 Hz, phenyl), 129.7 (s, phenyl), 127.3 (virtual t, J_{PC} = 5.0 Hz, phenyl), 124.5 (s, catechol), 122.9 (virtual t, J_{PC} = 18.9 Hz, catechol), 119.9 (virtual t, J_{PC} = 28.9 Hz, catechol), 110.7 (broad m, catechol). ^{31}P{^{1}H} NMR (36.3 MHz, d_7-DMF): δ 12.89 (s). IR (KBr): C−H bending 1473 cm^{-1}, $\upsilon_{(C-O-Ti)}$ 1253, 1264 cm^{-1}. Anal. Calcd for $Cs_4Ti_2C_{108}H_{78}P_6O_{12}Pd_3I_6$: C, 37.47; H, 2.27. Found: C, 37.40; H, 2.18.

$Cs_4[Sn_2L_6Pd_3I_6]$. Addition of CsI (468 mg, 1.80 mmol) to 20 mL of DMF solution of $Cs_4[Sn_2L_6Pd_3Br_6]$ (200 mg, 0.0602 mmol) resulted in a cloudy mixture that was stirred overnight. The mixture was filtered through a frit with Celite and glasswool, giving a dark-red filtrate that was evaporated in vacuo to give the product in quantitative yield (216 mg). Redissolving about 30 mg of the product in 10 mL of DMF gave a clear dark-red solution. Slow diffusion of diethyl ether into this solution gave well-formed dark-red crystals. ^{1}H NMR (360 MHz, d_7-DMF): δ 8.12 (td, J = 7.6 and 1.9 Hz, 6 × 1 cat-H), 7.66 (m, 6 × 4 phenyl-H), 7.35 (m, 6 × 6 phenyl-H), 6.67 (broad d, J = 7.9 Hz, 6 × 1 cat-H), 6.51 (broad m, 6 × 1 cat-H). ^{13}C{^{1}H} NMR (89.9 MHz, *d*-DMF): δ 156.1 (s, catechol), 151.3 (virtual t, J_{PC} = 9.3 Hz, catechol), 137.4 (virtual t, J_{PC} = 25.2 Hz, phenyl), 134.6 (virtual t, J_{PC} = 5.3 Hz, phenyl), 129.6 (s, phenyl), 127.4 (virtual t, J_{PC} = 4.6 Hz, phenyl), 125.3 (virtual t, J_{PC} = 11.3 Hz, catechol), 123.9 (s, catechol), 117.0 (m, catechol), 113.0 (m, catechol). ^{31}P{^{1}H} NMR (36.3 MHz, d_7-DMF) δ 12.25 (s). IR (KBr): C−H bending 1474, 1487 cm^{-1}, $\upsilon_{(C-O-Sn)}$ 1254 cm^{-1}. Anal. Calcd for $Cs_4Sn_2C_{108}H_{78}P_6O_{12}Pd_3I_6$: C, 36.00; H, 2.18. Found: C, 35.96; H, 2.12.

Self -Assembly of (NH$_4$)$_4$[$Ti_2Pd_3Br_6L_6$]. A suspension of $Ti(OMe)_4$, PPh_2-Catechol·HBr, $PdBr_2$·2PhCN, and NH_4OH in a molar ratio of 2:6:3:10 was stirred in degassed DMF under a nitrogen atmosphere at room temperature for a week giving a dark-red cloudy solution that was filtered through a frit filled with Celite and glasswool to give a dark-red filtrate. The filtrate was evaporated under vacuum to give a dark-red solid in over 80% yield. Redissolving about 20 mg of the product in 10 mL of DMF gave a clear dark-red solution. Slow diffusion of diethyl ether into this solution gave well-formed dark-red crystals of X-ray quality. ^{1}H NMR (360 MHz, d_7-DMF): δ 8.42 (broad m, 6 × 1 cat-H), 7.57 (broad, 6 × 4 phenyl-H), 7.34 (broad, 6 × 6 phenyl-H), 6.63 (broad d, J = 7.9 Hz, 6 × 1 cat-H), 6.40 (broad, 6 × 1 cat-H). ^{13}C{^{1}H} NMR (89.9 MHz, d_7-DMF): δ 156.3 (s, catechol), 151.7 (virtual t, J_{PC} = 8.0 Hz, catechol), 135.1 (virtual t, J_{PC} = 14.6 Hz, phenyl), 134.5 (broad, phenyl), 129.4 (broad, phenyl), 128.1 (broad, phenyl), 127.4 (broad, catechol), 125.2 (m, catechol), 125.0 (m, catechol), 113.7(broad, catechol). ^{31}P{^{1}H} NMR (36.3 MHz, d_7-DMF): δ 22.10 (s). IR (KBr): $\upsilon_{(NH4,\ N-H)}$ 3326 cm^{-1}, $\upsilon_{(aromatic\ C-H)}$ 3052, 3024 cm^{-1}; C−H bending 1468 cm^{-1}, $\upsilon_{(C-O-Ti)}$ 1259 cm^{-1}. Anal. Calcd for $Ti_2C_{108}H_{94}N_4P_6O_{12}Pd_3Br_6$: C, 47.69; H, 3.48; N, 2.06. Found: C, 47.52; H, 3.59; N, 2.17.

$Cs_4[Ti_2L_6\{Cr(CO)_4\}_3]$. A DMF (20 mL) solution of $Cs_2[TiL_3]$ (237 mg, 0.199 mmol) and $Cr(CO)_4$(piperidine)$_2$ (100 mg, 299 mmol) was stirred under a nitrogen atmosphere at room temperature for 7 days giving a clear orange-red solution. Addition of 50 mL of acetone precipitated a yellow solid, which was filtered off and washed with acetone (3 × 10 mL). The yellow solid was then dried under vacuum. Yield: 210 mg (66%). ^{1}H NMR (360 MHz, d_7-DMF): δ 7.76 (broad, 6 × 1 cat-H), 7.49 (broad, 6 × 4 phenyl-H), 7.38 (broad, 6 × 6 phenyl-H), 7.34 (broad, 6 × 1 cat-H), 6.14 (broad). ^{31}P{ ^{1}H} NMR (36.3 MHz, d_7-DMF): δ 72.09 (s). IR (KBr): $\upsilon_{(CO)}$ 1856 cm^{-1}; C−H bending 1474 cm^{-1}, $\upsilon_{(C-O-Ti)}$ 1260 cm^{-1}. Anal. Calcd for $Cs_4Ti_2C_{120}H_{78}P_6O_{24}Cr_3$: C, 50.16; H, 2.74. Found: C, 50.02; H, 2.79.

$Cs_4[Sn_2L_6\{Cr(CO)_4\}_3]$. A DMF (20 mL) solution of $Cs_2[SnL_3]$ (251 mg, 0.199 mmol) and $Cr(CO)_4$(piperidine)$_2$ (100 mg, 0.299 mmol) was stirred under a nitrogen atmosphere at room temperature for 7 days giving a clear orange-red solution. Addition of 50 mL of acetone

precipitated a yellow solid, which was filtered off and washed with acetone (3 × 10 mL). The yellow solid was then dried under vacuum. Yield: 230 mg (74%). ^{1}H NMR (360 MHz, d_7-DMF): δ 7.71 (broad m, 6 × 1 cat-H), 7.50 (broad, 6 × 4 phenyl-H), 7.39 (broad, 6 × 6 phenyl-H), 6.46 (broad d, J = 4.0 Hz, 6 × 1 cat-H), 6.15 (broad, 6 × 1 cat-H). ^{13}C{^{1}H} NMR (89.9 MHz, d_7-DMF): δ 155.0 (s, catechol), 152.7 (virtual t, 9.0 Hz, catechol), 140.2 (virtual t, 5.6 Hz, phenyl), 132.6 (virtual t, 4.6 Hz, phenyl), 128.8 (s, phenyl), 128.4 (m, phenyl), 128.0 (virtual t, 4.0 Hz, catechol), 121.4 (m, catechol), 120.3 (m, catechol), 112.8(m, catechol). ^{31}P{^{1}H} NMR (36.3 MHz, d_7-DMF): δ 71.55 (s). IR (KBr) $\upsilon_{(CO)}$ 1855 cm^{-1} , C−H bending 1477 cm^{-1}, $\upsilon_{(C-O-Sn)}$ 1251 cm^{-1}. Anal. Calcd for $Cs_4Sn_2C_{120}H_{78}P_6O_{24}Cr_3$: C, 47.81; H, 2.61. Found: C, 48.00; H, 2.65.

X-ray Crystal Structure Analysis. Experimental crystal data for **$Cs_4[Sn_2Pd_3Br_6L_6]$** and **$Cs_4[Ti_2Pd_3Br_6L_6]$** have been reported previously.[36] Crystal data for the other two structures reported herein were collected by using a Siemens SMART[76] diffractometer equipped with a CCD area detector with Mo Kα (λ = 0.71073 Å) radiation. Data in the frames corresponding to an arbitrary hemisphere of data were integrated by using SAINT.[77] Data for both structures were corrected for Lorentz and polarization effects. An empirical absorption correction based on the measurement of redundant and equivalent reflections and an ellipsoidal model for the absorption surface was applied with use of SADABS.[78] The structure solution and refinement for both structures was performed by using the teXsan[79] crystallographic software package (refining on F). Hydrogen atoms were included but not refined. Crystallographic data (excluding structure factors) have been deposited with the Cambridge Crystallographic Data Centre as supplementary publication numbers 139110 ((DABCO-H)$_4$[$Sn_2Pd_3Br_6$**L**$_6$]) and 139159 (Cs_2[Ti**L**$_3$]). Copies of the data can be obtained free of charge on application to The Director, CCDC, 12 Union Road, Cambridge CB21EZ, UK (fax: international code + (1223)336-033; e-mail: deposit@chemcrys.cam.ac.uk).

Acknowledgment. We thank the National Science Foundation (CHE-9709621), NSF/NATO (exchange grant INT-9603212/SRG951516), and Research Corporation (Research Opportunity Grant to E.H.W.) for financial support. We also thank Dr. Frederick J. Hollander for assistance with the crystallography and Dr. Martin Michels for helpful discussions and a thorough review of the manuscript.

Supporting Information Available: The X-ray structure reports of (DABCO-H)$_4$[$Sn_2Pd_3Br_6$**L**$_6$] and Cs_2[Ti**L**$_3$] (including tables of crystal data, data collection parameters, and discussions on modeling of the disorder in the molecules) (PDF). This material is available free of charge via the Internet at http://pubs.acs.org.

JA0029376

(76) *SMART, Area Detector Software Package*; Siemens Industrial Automation, Inc.: Madison, 1995.

(77) *SAINT, SAX Area Detector Integration Program*, 4.024 ed.; Siemens Industrial Automation, Inc.: Madison, 1995.

(78) Sheldrick, G. *SADABS, Siemens Area Detector ABSorption Correction Program*; Advanced Copy ed.; Personal Communication, 1996.

(79) *teXsan, Crystal Structure Analysis Package*; Molecular Structure Corporation: The Woodlands, TX, 1992.